J. Fluid Mech. (1965), *vol.* 23, *part* 1, *pp.* 31–64
Printed in Great Britain

The structure of a self-preserving turbulent plane jet

By L. J. S. BRADBURY†
Queen Mary College, University of London

(Received 26 January 1965)

The structure of a self-preserving turbulent plane jet exhausting into a slow-moving parallel airstream is studied. The investigation includes results of turbulence measurements and the structure is compared with that of a self-preserving plane wake. The results show that self-preservation is established at a distance of about thirty jet widths downstream of the jet nozzle and that, in the self-preserving region of the jet, the distributions of the turbulent intensities and shear stress across the jet are very similar to those found in the plane wake. The distribution of the intermittency factor, however, is found to be more like that found in an axi-symmetric jet than in a plane wake. The turbulent energy balance also shows important differences to that of the wake flow. The unsteady irrotational flow outside the turbulent shear layer is investigated and it is found that the experimental results agree with the predictions of the theories of Phillips (1955) and Stewart (1956). Some comments are also made on the eddy structure and the applicability of the simple theories of turbulence.

1. Introduction

The simplest types of turbulent shear flows are those of the self-preserving type in which the structure of the shear layer is similar at all streamwise stations. These flows may be subdivided into the bounded flows such as channel flows and boundary layers, and the unbounded flows such as jets and wakes. It is with this latter group that the present work is concerned. Although Townsend (1956) and Grant (1958) have studied extensively the structure of the self-preserving plane wake, the situation in regard to jet flows is not so satisfactory. Corrsin and his co-workers have carried out a large number of investigations into the axi-symmetric jet exhausting into a stationary atmosphere, but some of these measurements have been adversely affected by the high turbulence levels encountered and the non-linear response of the hot-wire anemometers used. Moreover, for comparison with Townsend's wake investigations, measurements in a plane jet would be preferred. The most important reports on this flow are those of Forthmann (1936), Miller & Commings (1957), van der Hegge Zijnen (1958*a*, *b*, *c*) and Nakaguchi (1961). Unfortunately, none of these investigations were comparable in detail to Townsend's work on the wake, and the present work was undertaken to provide more information about this flow than was hitherto available.

The condition for self-preservation of a plane jet is that the jet velocity on the

† Now at the Royal Aircraft Establishment, Farnborough, Hampshire.

centre-line of the flow must be much greater than the free-stream velocity and this condition has been achieved in the past by the obvious expedient of carrying out measurements in a plane jet exhausting into a stationary atmosphere. However, this has the disadvantage that the turbulent intensities at the edge of the jet are very high which leads invariably to large errors in the measurements. In the present experiments, this problem was largely avoided by having the jet exhaust into a comparatively slow-moving airstream. This flow cannot be exactly self-preserving but the departure from self-preservation in the region in which measurements were made was found to be small and of no significance.

The distributions across the jet of mean velocity, static pressure, intermittency factor and the turbulent intensities and shear stress have been measured in the self-preserving region of the flow. Also, the turbulent energy balance has been computed and the results of a tentative study of the eddy structure are reported. The results of these various measurements are compared in some detail with the corresponding results for the plane wake flow. Some measurements have also been made in the irrotational flow outside the turbulent jet and comparisons are made with the theories of Phillips (1955) and Stewart (1956). Finally, the applicability of the various simple theories of turbulence is discussed.

2. Equations of motion and self-preservation

Only two-dimensional flows will be considered. Cartesian co-ordinates will be used with the x-axis and y-axis lying parallel and normal to the free-stream direction respectively. The longitudinal or x-component of mean velocity will be denoted by U and the lateral or y-component by V. The turbulent velocities will be denoted as usual by u, v and w. The equations of motion for a free two-dimensional shear layer with 'boundary layer' assumptions are

$$U\frac{\partial U}{\partial x}+V\frac{\partial U}{\partial y}=-\frac{\partial \overline{uv}}{\partial y}-\frac{\partial(\overline{u^2}-\overline{v^2})}{\partial x}, \tag{1}$$

$$P_1=P+\overline{\rho v^2}, \tag{2}$$

where P is the static pressure and the suffix 1 refers to free-stream conditions. The continuity equation is

$$\partial U/\partial x+\partial U/\partial y=0. \tag{3}$$

Following Townsend (1956), we may consider self-preserving flows in which

$$U=U_1+U_0 f(y/\delta);\quad \overline{uv}=U_0^2 g_{12}(y/\delta);\quad \overline{u^2}=U_0^2 g_1(y/\delta);\quad \overline{v^2}=U_0^2 g_2(y/\delta). \tag{4}$$

U_0 is taken as the mean velocity difference between the centre-line of the shear flow and the free-stream and δ is some relevant length scale of the shear layer which will be defined in the present work as the y-ordinate at which $U=U_1+\frac{1}{2}U_0$ (see figure 1); f, g_{12}, g_1 and g_2 are all functions of $\eta=y/\delta$ only. Substituting these expressions into equation (1) gives

$$\frac{U_1}{U_0}\left[\frac{\delta}{U_0}\frac{dU_0}{dx}f-\frac{d\delta}{dx}\eta f'\right]+\frac{\delta}{U_0}\frac{dU_0}{dx}f^2-\frac{1}{U_0}\frac{d}{dx}(\delta U_0)f'\int_0^\eta f\,d\eta$$
$$+2\frac{\delta}{U_0}\frac{dU_0}{dx}(g_1-g_2)-\frac{d\delta}{dx}\eta(g_1'-g_2')+g_{12}'=0. \tag{5}$$

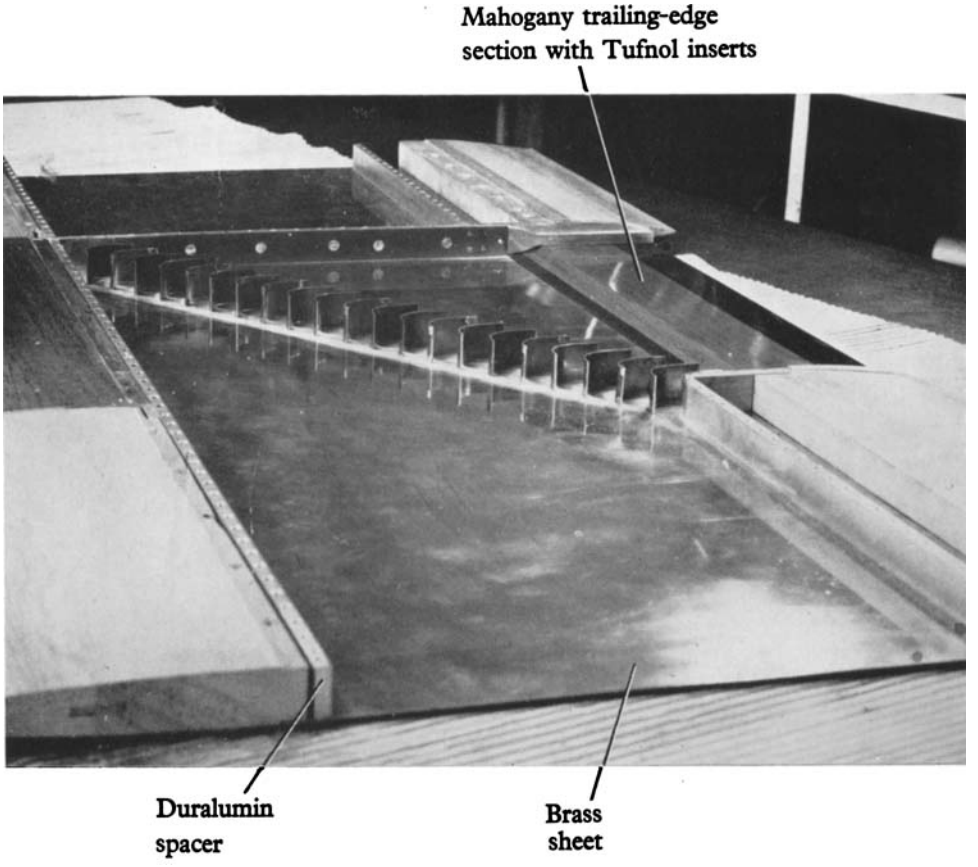

FIGURE 3. Jet model with brass top plate removed.

To be consistent with the assumption of self-preservation, it is necessary that the coefficients in equation (5) are in constant ratio to one another. With the use of the momentum integral equation, this leads to the following conditions (see Townsend 1956):

(i) When $U_0 \gg U_1$, $\delta \propto x$ and $U_0 \propto x^{-\frac{1}{2}}$. This is the plane jet flow in a slow-moving airstream when the velocity on the centre-line of the jet is much greater than the free-stream velocity.

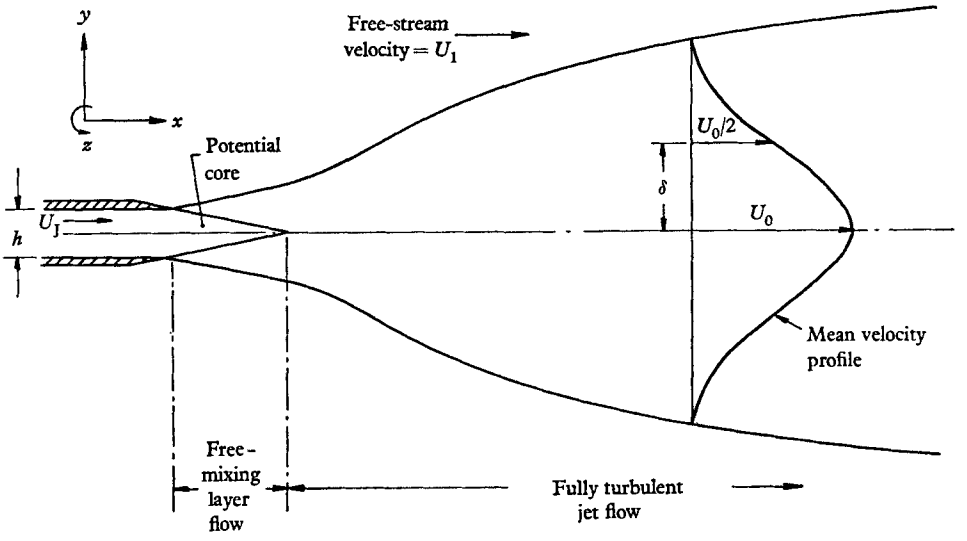

FIGURE 1. Schematic representation of the flow.

(ii) When $U_0 \ll U_1$, $\delta \propto x^{\frac{1}{2}}$ and $U_0 \propto x^{-\frac{1}{2}}$. This represents either a plane wake far downstream from the cylinder producing the wake or, alternatively, a plane jet flow in a moving airstream when the velocity on the jet centre-line is approaching the free-stream velocity.

(iii) When $U_0 = U_1 = \text{const.}$, $\delta \propto x$. This is the free-mixing layer between two parallel streams.

In this note, we are concerned with the first of these flows. The condition for self-preservation that $U_0 \gg U_1$ has been obtained in the past by exhausting the jet into a stationary atmosphere, i.e. $U_1 = 0$. However, as mentioned in the introduction, this has some serious disadvantages and, in the present experiments, the jet exhausted into a comparatively slow-moving airstream. In this way, the turbulent intensities relative to the local mean velocity were greatly reduced.

The shear stress was measured with a hot-wire anemometer and also calculated from the mean velocity measurements using equation (5), which may be integrated to give

$$-\frac{\overline{uv}}{U_0^2} = -g_{12} = \left(\frac{U_1}{U_0}\right)\left[\frac{\delta}{U_0}\frac{dU_0}{dx}+\frac{d\delta}{dx}\right]\int_0^\eta f\,d\eta - \frac{U_1}{U_0}\frac{d\delta}{dx}\eta f$$
$$+\left[2\frac{\delta}{U_0}\frac{dU_0}{dx}+\frac{d\delta}{dx}\right]\int_0^\eta f^2\,d\eta - \left[\frac{\delta}{U_0}\frac{dU_0}{dx}+\frac{d\delta}{dx}\right] f\int_0^\eta f\,d\eta. \qquad (6)$$

The terms containing the functions g_1 and g_2 are small and have been ignored. This simplification has been checked by using measured values of the functions g_1 and g_2.

In the case when $U_1 = 0$, it is easy to show that equation (6) simplifies to

$$-g_{12} = -\frac{1}{2}\frac{d\delta}{dx} f \int f d\eta. \tag{7}$$

The inflow into jets is also of interest and calculations of the mean lateral velocity have been made (§ 4.1). From the continuity equation, it is found that

$$V = -\int \frac{dU}{dx} dy = -\delta \frac{dU_0}{dx} \int_0^\eta f d\eta + U_0 \frac{d\delta}{dx} \int_0^\eta \eta f' d\eta,$$

so that

$$\frac{V}{U_0} = -\frac{\delta}{U_0}\frac{dU_0}{dx} \int_0^\eta f d\eta + \frac{d\delta}{dx}\left(\eta f - \int_0^\eta f d\eta\right). \tag{8}$$

Again when $U_1 = 0$, this becomes

$$\frac{V}{U_0} = \frac{d\delta}{dx}\left(\eta f - \frac{1}{2}\int_0^\eta f d\eta\right). \tag{9}$$

3. Experimental apparatus and techniques

The apparatus consisted basically of a thin wing spanning horizontally the 4 ft. × 3 ft. closed return tunnel at Queen Mary College, with a jet nozzle consisting of a slot 18 in. × $\frac{3}{8}$ in. extending over the centre 18 in. of the trailing edge of the wing (figure 2). The wing shown in figure 3 (plate 1) had a chord of 26 in. and was approximately 1 in. thick. The air supply for the jet was provided by a centrifugal fan which supplied the air to the jet via a duct within the wing. The duct ran parallel to the span of the wing with a rectangular cross-section 13 in. × 1 in. At the wing centre the duct formed a right-angled bend expanding out to a section 18 in. × 1 in. On this bend twenty-three corner-vanes were provided to ensure an even distribution of velocity at the jet exit. Finally, at the trailing edge the duct contracted smoothly to a thickness of $\frac{3}{8}$ in. to form the trailing-edge jet. For the mixing of the jet- and mainstream-flow to be as closely two-dimensional as possible, two plywood walls were mounted in the tunnel parallel to the mainstream as shown in figure 2.

The variation of total head across the span of the jet (at the jet nozzle) was within 1 % of the mean value. However, 25 in. downstream (which was about the farthest point at which measurements could be made), the distribution had developed the 'saddleback' form found by van der Hegge Zijnen (1958*a*). Even so, over the centre 10 in. of the jet, the variation of total head was less than 4 %.

The traversing gear enabled the measuring instruments to be traversed both laterally across the jet and longitudinally in the direction of the free-stream. *Mean velocity and static pressure measurements were made with separate Pitot* and static tubes of 0·05 in. diameter. The turbulence measurements were made with constant-current, 0·0001 in. diameter platinum hot-wire anemometers. Although the hot-wire anemometer equipment was of conventional design, con-

siderable care was taken over its design and development to ensure that measurements were both reliable and accurate (see Bradbury 1963).

The turbulent intensities encountered were generally low enough to ignore the effect of the turbulence on the mean velocity measurements with the separate Pitot and static tubes. However, in the case of the measurement of the static

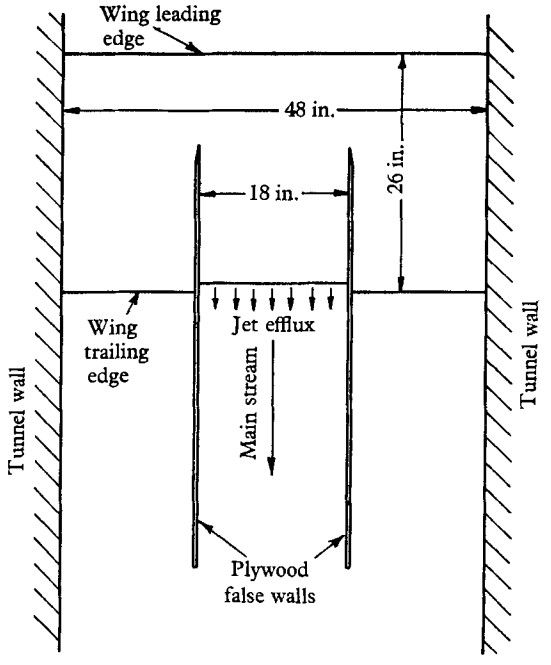

FIGURE 2. Plan view of jet wing in the tunnel.

pressure coefficient, $(P-P_1)/\rho U_0^2$, the effect of the turbulence can easily be shown to be significant. Equation (2) gives for the true static pressure coefficient

$$\Delta P/\rho U_0^2 = (P-P_1)/\rho U_0^2 = -\overline{v^2}/U_0^2.$$

Now, for the static tube reading P_S, it is usual to assume that

$$P_S = P + \tfrac{1}{2}\rho n(\overline{v^2}+\overline{w^2}),$$

where n is a factor to allow for the effect of the turbulence and which can take positive or negative values depending on the scale of the turbulence, with limiting values of $+1$ and -1 respectively (see Toomre 1960 and Bradbury 1963). Therefore, the measured static pressure coefficient can be written

$$\frac{\Delta P_S}{\rho U_0^2} = \frac{P_S-P_1}{\rho U_0^2} = -\frac{\overline{v^2}}{U_0^2} + \tfrac{1}{2}n\left(\frac{\overline{v^2}}{U_0^2}+\frac{\overline{w^2}}{U_0^2}\right).$$

This expression clearly shows that it is possible for the measured and true static pressure coefficients to differ considerably from one another. Lack of precise information about the dependence of the factor n on the scale of the turbulence in relation to the static tube diameter precludes corrections being made to the

measurements; but it would seem that, in a self-preserving flow, the measured static pressure coefficients will also be self-preserving provided the factor n does not alter appreciably from one longitudinal station in the flow to another. Thus, static pressure measurements can provide a simple means of studying how rapidly a flow approaches self-preservation.

In order to calculate the turbulent intensities from the hot-wire anemometer measurements, use was made of the heat-transfer law proposed by Collis & Williams (1959). In terms of practical parameters, this law may be written

$$i^2R_H/(T_H-T_1) = A[1+\Omega(T_H-T_1)]+B[1+\Pi(T_H-T_1)]\,U^mS(\psi), \qquad (10)$$

where i is the current through the wire, R_H is the hot-wire resistance, T_H and T_1 are the hot-wire and ambient temperatures respectively, and U is the air velocity. A and B are constants for a given wire and ambient temperature. The parameters Ω and Π are only weakly dependent on the ambient temperature and can be regarded as absolute constants over the range of ambient temperatures normally encountered. According to Collis & Williams

$$\Omega = 0{\cdot}00164 \quad \text{and} \quad \Pi = 0{\cdot}00025 \text{ at } T_1 = 293\,^\circ\text{K}.$$

The power m is 0·45 at the wire Reynolds number encountered in the present experiments. $S(\psi)$ is a function of the angle between the wire and the flow direction ψ, and represents the effect of yaw on the heat transfer. According to experiments of Webster (1962), this function may be written

$$S(\psi) = \sin^m\psi(1+0{\cdot}04\cot^2\psi)^{\frac{1}{2}m}. \qquad (11)$$

In a note by Ruetnik (1955) it was found that the effect of the second temperature coefficient of resistance in the calculation of turbulent intensities was not necessarily negligible, and its effect was therefore included in the present work. Following the usual linearization technique (see, for example, Newman & Leary 1949), equations (10) and (11), after a good deal of manipulation, give for constant current operation

$$\frac{-i}{i^2-i_0^2}\frac{R_1}{R_H(R_H-R_1)}(1+\phi)\,e = \frac{mu}{U}+m\cot\psi\left[1-\frac{0{\cdot}04}{\sin^2\psi(1+0{\cdot}04\cot^2\psi)}\right]\frac{v}{U}, \qquad (12)$$

where i, R_H, U and ψ are now mean values and where e is the change in voltage across the wire due to the turbulent velocities u and v. i_0 is the current at $U=0$ obtained from equation (10), and R_1 is the resistance of the wire at ambient temperature. Also

$$\phi = \frac{R_H}{R_1}\frac{R_H-R_1}{R_0}\left[\frac{i_0^2}{i^2}\frac{\Omega}{\alpha}\frac{1}{1+\Omega(R_H-R_1)/\alpha R_0}+\frac{i^2-i_0^2}{i^2}\frac{\Pi}{\alpha}\frac{1}{1+\Pi(R_H-R_1)/\alpha R_0}-\frac{\beta}{\alpha^2}\right],$$

where α and β are the first and second temperature coefficients of resistance, respectively, and R_0 is the wire resistance at 0 °C (273 °K). Equation (12) is similar in form to that obtained by Ruetnik using King's law and differs from the more usual expressions by the inclusion of the $(1+\phi)$ term. This term can be important and, if it is ignored, errors may result of about 20–30 % in the values of

$\overline{u^2}$, say. As pointed out by Ruetnik, the β/α^2 term in the expression for ϕ is positive for tungsten and negative for platinum, taking the respective values of $+0{\cdot}026$ and $-0{\cdot}045$.

The application of equation (12) to practical measurements follows conventional procedure and is adequately described by, say, Newman & Leary (1949).

4. Experimental results

The tests were carried out with two ratios of free-stream to jet velocity, namely with $U_1/U_J = 0{\cdot}07$ and $U_1/U_J = 0{\cdot}16$.† In both cases, the Reynolds number based on jet velocity U_J, and nozzle width h, was about 3×10^4. In the tests with $U_1/U_J = 0{\cdot}07$, the value of U_0/U_1 varied from 13·3 at the jet nozzle to about 4 at $x/h = 70$, so that the condition for self-preservation, $U_0 \gg U_1$, was reasonably well fulfilled throughout the region in which measurements were made. However, turbulent intensities at the edge of the jet were still too high to enable accurate measurements to be made, and consequently the bulk of the tests were carried out with $U_1/U_J = 0{\cdot}16$. In this case, U_0/U_1 was only about 1·7 at $x/h = 70$, which shows that the condition for self-preservation, $U_0 \gg U_1$, was not properly maintained. However, by comparison with the results when $U_1/U_J = 0{\cdot}07$, there is no doubt that, in all major details, the results with $U_1/U_J = 0{\cdot}16$ are representative of a truly self-preserving jet. The departures from self-preservation that were found will be discussed later as they arise and the detailed results with $U_1/U_J = 0{\cdot}07$ will not be presented.

4.1. *The mean velocity field*

The mean velocity profiles were measured with separate Pitot and static tubes. These profiles in the fully turbulent region of the jet were all found to be geometrically similar as shown in figure 4 and a good empirical fit to them is given by

$$f(\eta) = \exp[-0{\cdot}6749\eta^2(1+0{\cdot}0269\eta^4)]. \tag{13}$$

Compared with previously measured mean velocity profiles in a plane jet, the present results show a slightly more rapid approach to the free-stream velocity and the profile is not very different from that found by Townsend in a plane wake.‡

A check on the constancy of the momentum flux has been made using the results for the spread of the jet and the decay of the centre-line velocity shown in figure 5. The momentum integral equation is

$$\rho \int_{-\infty}^{\infty} U(U-U_1)\,dy = J, \text{ the excess momentum flux } (= \text{a constant}); \tag{14}$$

from this we may define a momentum coefficient

$$C_J = J/\rho U_1^2 h = \delta/h[(U_0/U_1)^2 I_2 + (U_0/U_1) I_1], \tag{15}$$

† With the wind-tunnel motor switched off, the jet induced a small flow around the closed circuit of the tunnel. Under these conditions, the value of $U_1/U_J = 0{\cdot}07$ was obtained and this value was therefore the lowest value obtainable.

‡ The expression of Townsend (1956, p. 161) in terms of the reference length, δ, used in this note is $f(\eta) = \exp[-0{\cdot}6619\eta^2(1+0{\cdot}0565\eta^4)]$.

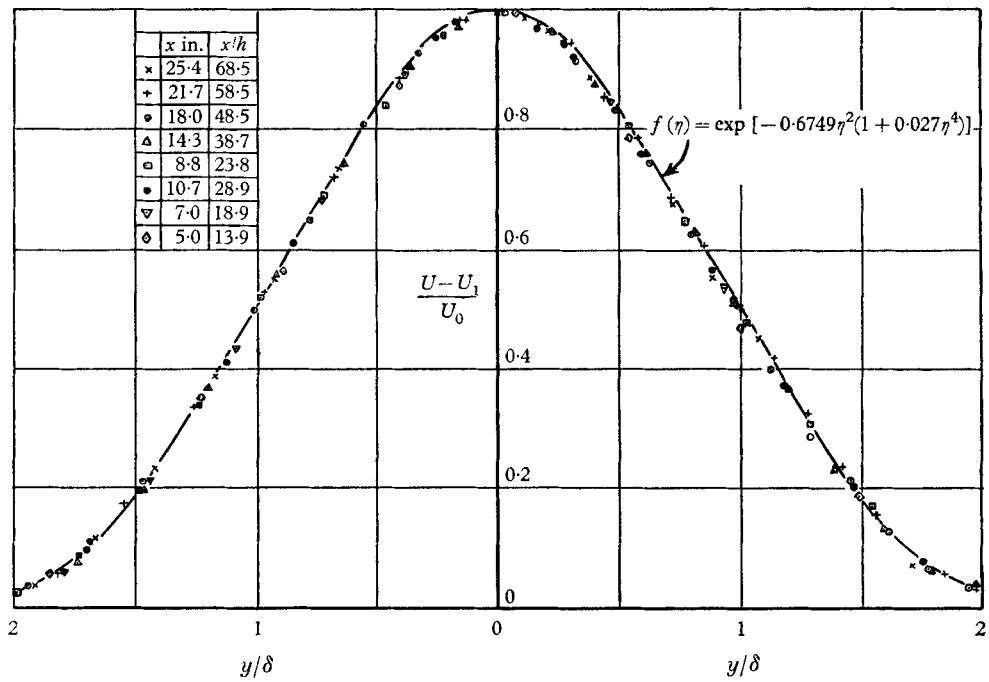

FIGURE 4. Mean velocity profiles in the fully turbulent jet.

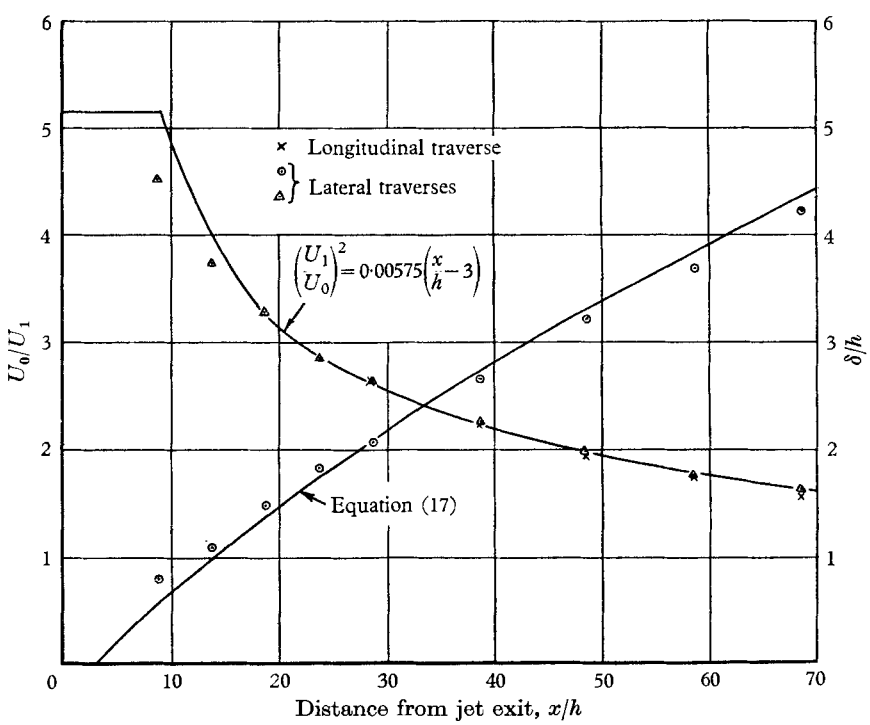

FIGURE 5. Variation of jet width and centre-line velocity.

where $I_n = \int_{-\infty}^{\infty} f^n(\eta)\, d\eta$. Using the results shown in figure 5 and the mean velocity profile function $f(\eta)$, it was found that the deviation from the average value of $C_J = 31{\cdot}5$ was less than 4% at each of the longitudinal measuring stations.

The condition for self-preservation that $U_0 \propto x^{-\frac{1}{2}}$ is well observed. An expression which fits the experimental data is

$$(U_1/U_0)^2 = C(x/h - x_0/h), \tag{16}$$

where, in this particular case, $C = 0{\cdot}00575$ and $x_0/h = 3$. Although the values of the constants in this expression have no general significance, it is worth noting that using this expression in the momentum integral equation gives

$$\frac{\delta}{h} = \left(\frac{U_1}{U_0}\right)^2 \frac{C_J}{I_2} \frac{1}{(1 + U_1 I_1/U_0 I_2)} = \frac{0{\cdot}123(x/h - x_0/h)}{1 + 0{\cdot}0755(x/h - x_0/h)^{\frac{1}{2}}}. \tag{17}$$

This expression which is also shown in figure 5 shows that if $U_0 \propto x^{-\frac{1}{2}}$, the spread of the jet cannot now be exactly proportional to x as is required for self-preservation. However, this departure from true self-preservation is small in the present case and is of no great significance.

Lateral mean velocity profiles have been calculated using equation (8) for $x/h = 20$ and 60. These are compared in figure 6 with the profile obtained for a jet exhausting into still air with a rate of spread given by

$$d\delta/dx = 0{\cdot}109.$$

This value for the rate of spread was obtained from the tests with $U_1/U_J = 0{\cdot}07$ by comparing calculated shear-stress profiles at this velocity ratio with those obtained for a jet in still air using equation (7). The lateral mean velocity profiles in figure 6 are all broadly similar although departures from both the still-air profile and self-preservation are apparent.

It is also worth noting that the inflow angle at the edge of the jet,

$$\tan^{-1}(V/U) \approx V/U,$$

in the present tests was much less than in a jet with $U_1 = 0$ (see figure 7). This reduction of inflow angle suggests that the present measurements should be more accurate in this region of the flow than in previous experiments with $U_1 = 0$.

One further comment on the mean velocity results is necessary. When the free-stream velocity is finite, fluid particles that leave the jet nozzle arrive at a given value of x/h more rapidly than in a jet exhausting into still air, i.e. the free-stream tends to 'sweep' the jet along. This effect is important when comparing the approach to self-preservation found in the present tests with that found previously in tests with $U_1 = 0$ and, in order to obtain some idea about its magnitude, the time taken for a particle travelling with the jet centre-line velocity to reach a given value of x/h has been calculated for both $U_1 = 0$ and $U_1 \neq 0$. This time, which subsequently will be referred to as the 'existence' time, is given by

$$t_e = \int_0^x \frac{dx}{U_1 + U_0}. \tag{18}$$

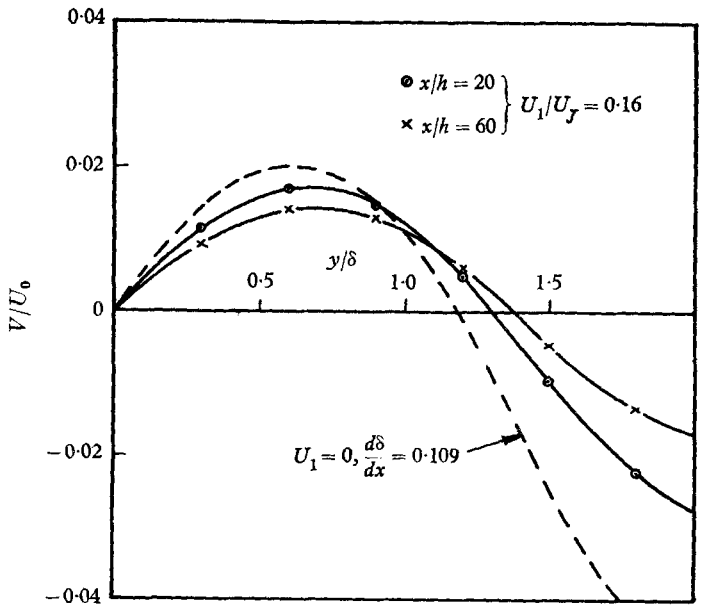

FIGURE 6. The lateral mean velocity profiles.

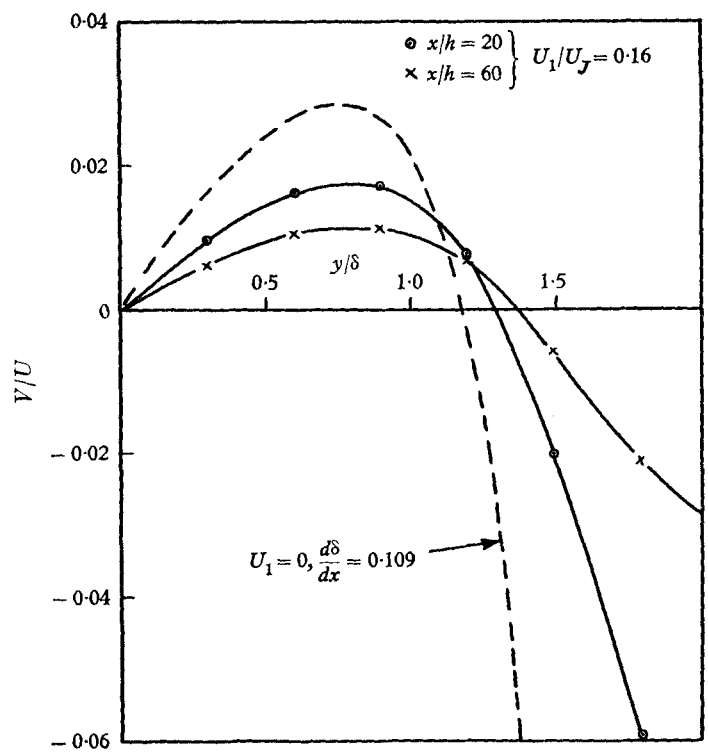

FIGURE 7. Ratio of lateral to longitudinal mean velocity across the jet.

In the self-preserving region of a plane jet exhausting into still air

$$\{\rho U_0^2(x-x_0)/J\}^{\frac{1}{2}} = C \quad (= \text{a constant}), \tag{19}$$

where J is the jet momentum flux and x_0 is the shift in the apparent origin of the flow due to the time taken to establish self-preservation. It is found that this expression is also in good agreement with experimental results for jets in slow-moving airstreams, provided J is taken to be the excess jet momentum flux.† For a jet with a uniform velocity U_J across the jet nozzle

$$J = \rho U_J(U_J - U_1)h,$$

and equation (19) becomes

$$U_0/\{U_J(U_J-U_1)\}^{\frac{1}{2}} = C/\{x/h - x_0/h\}^{\frac{1}{2}}. \tag{20}$$

If we consider regions sufficiently far downstream so that $x/h \gg x_0/h$ then equations (18) and (20) give

$$\frac{U_J t_e}{h} = \frac{2}{U_1/U_J}\left[\frac{1}{2}\frac{x}{h} - K\left(\frac{x}{h}\right)^{\frac{1}{2}} + K^2 \ln\left(1+\frac{(x/h)^{\frac{1}{2}}}{K}\right)\right], \tag{21}$$

where

$$K = C\left\{\frac{U_J}{U_1}\left(\frac{U_J}{U_1}-1\right)\right\}^{\frac{1}{2}}.$$

When $U_1 = 0$, this becomes

$$\frac{U_J t_e}{h} = \frac{2}{3C}\left(\frac{x}{h}\right)^{\frac{3}{2}}. \tag{22}$$

Using a value of $C = 2{\cdot}4$, which gives good agreement with experimental results, these last two relationships show that on an existence-time basis, the flow at $x/h = 70$ with $U_1/U_J = 0{\cdot}16$ is roughly equivalent to the flow at $x/h = 60$ with $U_1 = 0$. Thus, there is no serious stretching of the x-co-ordinate to be taken into account when comparing the approach to self-preservation in the present tests with that of previous work.

4.2. *Self-preservation of the turbulence structure*

The distributions across the jet of the static pressure coefficient at various longitudinal stations are shown in figure 8. The profiles are essentially similar for $x/h \geqslant 30$ and this suggests that, beyond this station, the turbulence structure is at least close to a state of self-preservation. The $\overline{u^2}/U_0^2$ profiles shown in figure 9 confirm this.

The variations of the static pressure coefficient and $\overline{u^2}/U_0^2$ along the centre-line of the jet are shown in figures 10 and 11 respectively. Also shown are the corresponding results obtained by previous experimenters for a jet in still air. The agreement between each set of data is comparatively poor and, although differences in magnitude could be due to the type of instrumentation used, even the trends are somewhat different. The present results show that self-preservation is established for $x/h \geqslant 30$, whereas previous experiments show that self-preservation

† This conclusion results from a more general investigation into the spread of a jet in a moving airstream, which will be reported more fully at some later stage.

does not occur at least until $x/h \geqslant 50$. No satisfactory explanation for these differences can be offered. However, the repeatability of the present results with different hot-wire anemometers was very good and the agreement between results with $U_1/U_J = 0{\cdot}07$ and $U_1/U_J = 0{\cdot}16$ was also excellent. In addition, some tests were made with the jet Reynolds number roughly halved but this had no effect on the results.

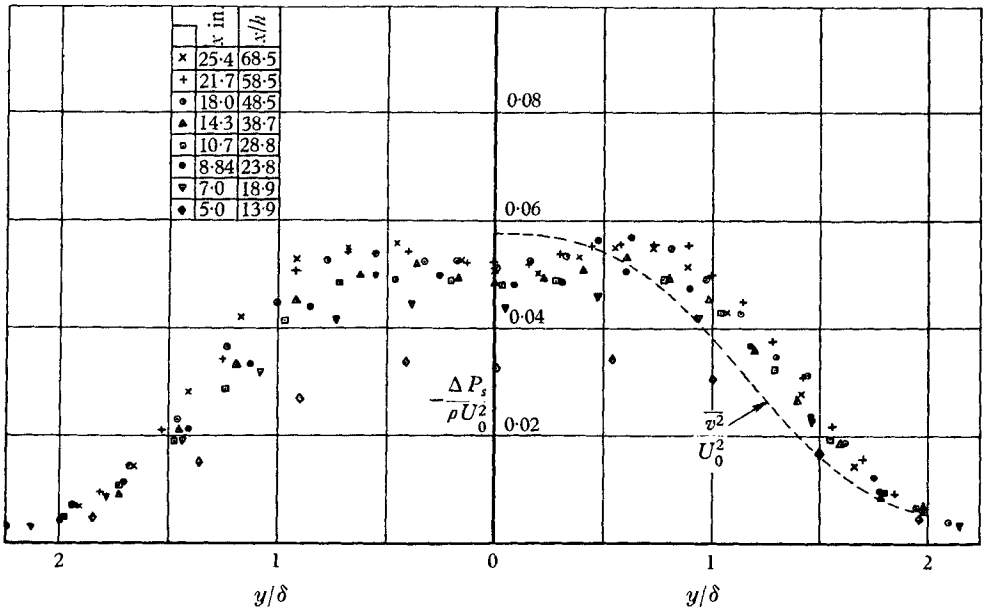

FIGURE 8. Static pressure-coefficient profiles.

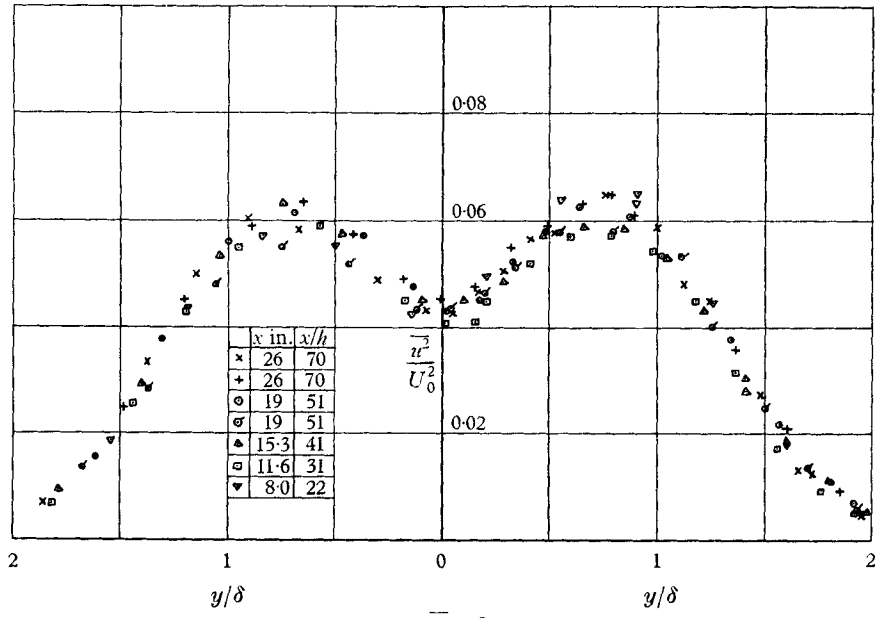

FIGURE 9. $\overline{u^2}/U_0^2$ profiles.

It is instructive at this stage to compare the approach to self-preservation of the plane jet with the plane wake. Townsend showed that self-preservation of the turbulence structure of a plane wake did not occur until the distance downstream from the circular cylinder was greater than 500 diameters, although the

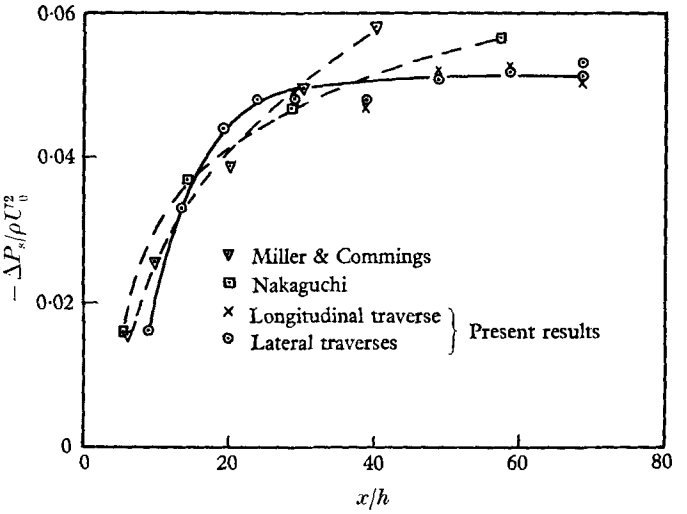

FIGURE 10. Variation of static pressure along the jet centre-line.

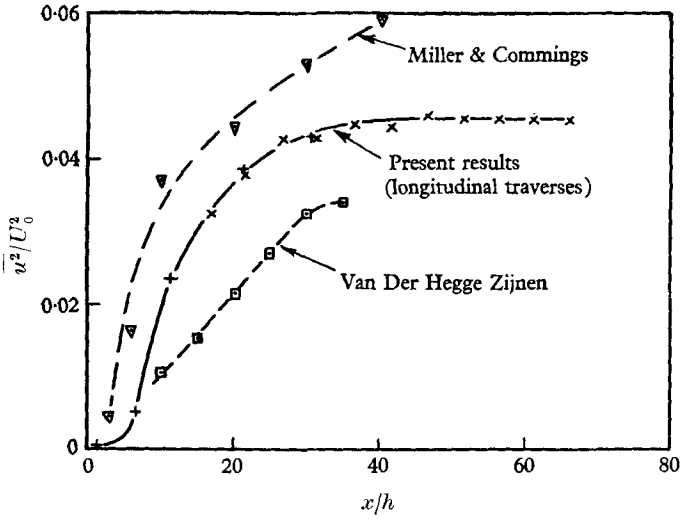

FIGURE 11. $\overline{u^2}/U_0^2$ variation along the jet centre-line.

main features of the self-preserving flow were established at roughly 200 diameters downstream. In the plane-jet case, the present work indicates that the flow is closely self-preserving for $x/h \geqslant 30$. A simple, though not necessarily precise, means of comparing the results for the two flows is on the existence-time basis. For a plane wake, Townsend (1956) obtained

$$U_1 t_e/d = 1{\cdot}1(x/d),$$

where d is the cylinder diameter. For the plane jet ($U_1 = 0$), we have

$$U_J t_e/h = 0{\cdot}28(x/h)^{\frac{3}{2}}.$$

Thus, for equal existence times

$$(x/h)^{\frac{3}{2}}_{\text{jet}} = 3{\cdot}95(x/d)_{\text{wake}}.$$

Using the results for the plane wake suggests that the structure of the plane jet should be approximately self-preserving for $x/h \geqslant 90$ and closely self-preserving for $x/h \geqslant 160$. These values are significantly larger than the value obtained from the present experiments. A likely cause for this difference is that the wake flow close to the circular cylinder contains a considerable excess of turbulent energy over the self-preserving wake and this excess will take a long time to decay. By contrast, the conditions at the nozzle of a plane jet are such that the turbulent energy is much less than that contained in the self-preserving jet and the approach to self-preservation is characterized by a production of turbulent energy up to, rather than by a process of decaying down to, the equilibrium self-preserving value. Although production and dissipation times for the turbulent energy are roughly similar (see Townsend 1956, p. 96), the difference between the turbulent energy close to the cylinder in the wake flow and far downstream in the self-preserving region of the flow is much greater than the difference in a plane jet between the conditions close to the jet nozzle and far downstream. This may well account for the somewhat different approaches to self-preservation of the wake and the jet. In this context, it would be interesting to study the approach to self-preservation of a wake flow behind a streamline body which did not generate the same excess of turbulent energy as the comparatively bluff circular cylinder.

4.3. *The intermittency factor*

The intermittency factor was measured directly on a simple instrument previously described (Bradbury 1964). Comparisons between these direct measurements and intermittency-factor results obtained from film recordings of hot-wire signals showed good agreement. Figure 12 shows distributions of intermittency factor across the jet which are broadly similar to those obtained by Corrsin & Kistler (1954) in an axisymmetric jet and, in consequence, they support Townsend's assertion that the large eddies in jets are smaller than those in wakes.

A point of interest is whether the essentially irrotational flow that exists between the turbulent 'bursts' has a mean velocity equal to the free-stream velocity or whether it is accelerated by pressure forces to have a mean velocity equal to that of the turbulent fluid. Direct measurements by Townsend in a wake flow indicate that the irrotational flow has essentially the same mean velocity as the turbulent fluid. On the other hand, some observations in a flat-plate turbulent boundary layer by Klebanoff (1954) of the output signals from a hot-wire anemometer seem to support the opposite view. It had been the intention in the present experiments to make some direct measurements on this matter, but equipment could not be developed in the time available. However, observations

of traces from the hot-wire output did not reveal any obvious correlation between a turbulent 'burst' and a rise in the 'mean velocity' of the sort observed by Klebanoff. It may be that, on this point, there is some difference between the free turbulent flows and the boundary-layer flows.

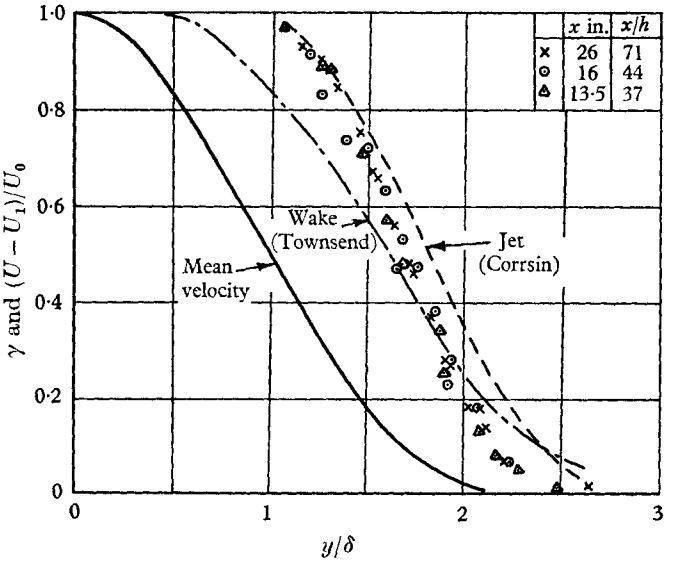

FIGURE 12. The intermittency factor.

4.4. *The distribution of the turbulent shear stress and intensities across a self-preserving plane jet*

As a result of the preceding work, subsequent measurements of the turbulence structure were restricted to two stations in the self-preserving region of the flow at $x/h = 50$ and $x/h = 70$. Measurements of the shear stress at these two stations are compared in figure 13 with the shear stress calculated from the momentum equation (§ 2). The agreement between the measured and calculated results is reasonable and provides a welcome check on the accuracy of the hot-wire measurements. It will be noted that the shear stress with $U_1/U_J = 0{\cdot}16$ is about 10 % larger than in a jet with $U_1 = 0$ and $d\delta/dx = 0{\cdot}109$. A possible explanation for this is that there is a reduction in the strain rate ratio $(\partial U/\partial x)/(\partial U/\partial y)$, in the outer region of the jet with $U_1/U_J = 0{\cdot}16$ as compared to the jet in still air and, according to Townsend's large-eddy hypothesis, this would lead to somewhat larger eddies and a corresponding increase in the eddy viscosity-coefficient. However, the difference in shear stress is not large and does not affect the general structure of the flow.

The $\overline{v^2}$ and $\overline{w^2}$ measurements were made with a single sloping hot-wire anemometer. This simple technique is inherently less accurate than the X-wire method so that the distributions of $\overline{v^2}$ and $\overline{w^2}$ are probably not as accurate as the $\overline{u^2}$ distributions. However, the results of these and the $\overline{u^2}$ measurements have been summarized in figures 14 and 15, which show the distributions of the three components of the turbulent motion and the turbulent energy $\overline{q^2} = \overline{u^2} + \overline{v^2} + \overline{w^2}$,

respectively, across the jet in the self-preserving region of the flow. By comparison with Townsend's wake measurements (Townsend 1956, pp. 142 and 143), it is clear that the distributions of these quantities across the plane jet are very similar

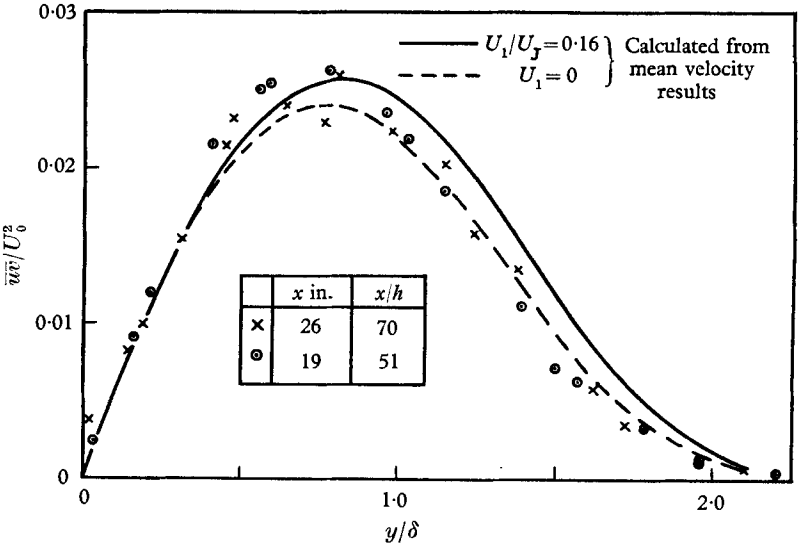

FIGURE 13. Shear-stress profiles.

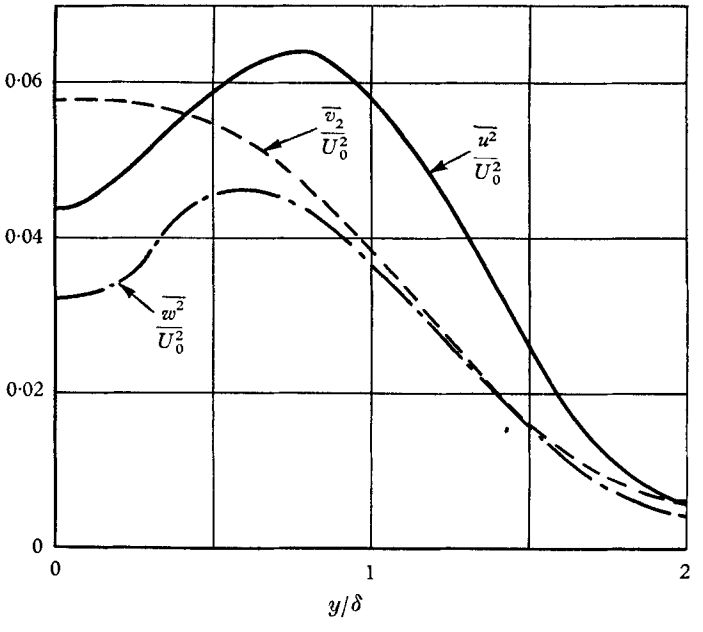

FIGURE 14. Distributions of turbulent intensities in a self-preserving jet.

to those in the plane wake, although they are, of course, different in magnitude. This similarity with the wake flow is better illustrated by the comparisons of the ratios of the turbulent intensities and shear stress in figures 16 and 17. The results for the two flows are in moderately good agreement with one another and

they show that, over the main portion of the flow, there is a measure of similarity in the turbulence structure although it is at best only a very rough similarity, i.e. the ratios of the turbulent intensities to one another and to the shear stress are roughly constant over a large portion of the shear-layer.

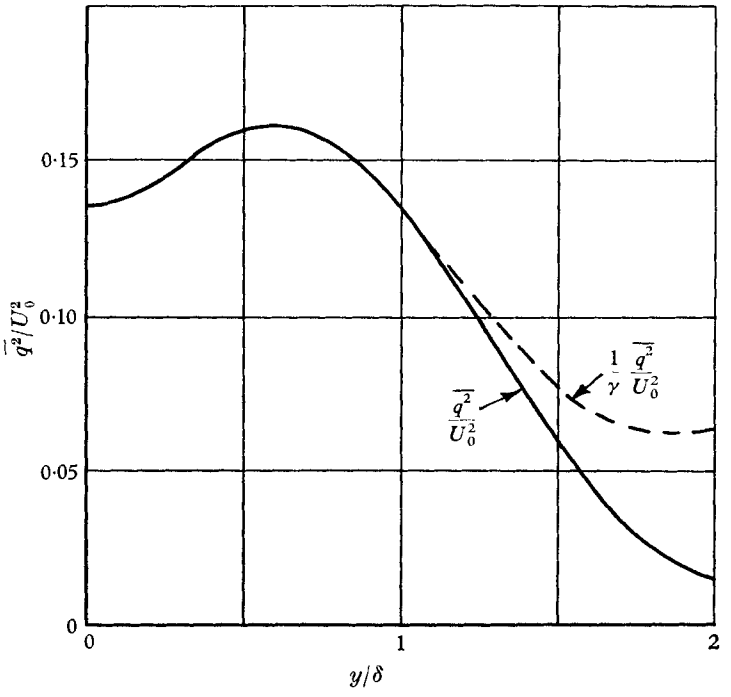

FIGURE 15. Turbulent energy distribution across a self-preserving jet.

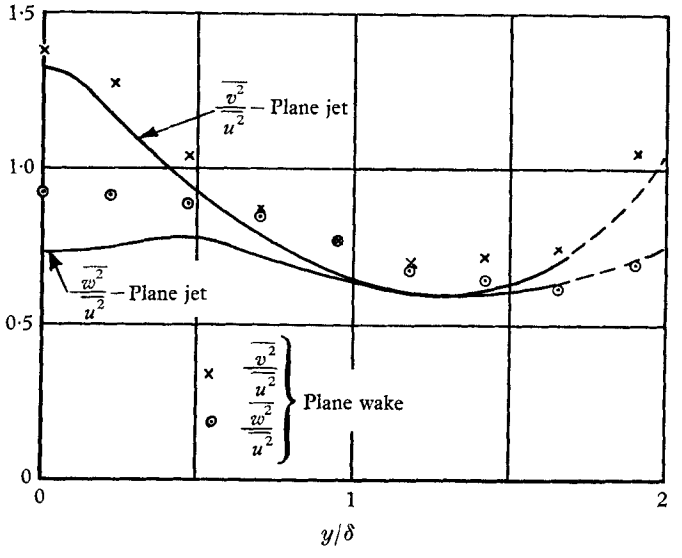

FIGURE 16. The ratios of the turbulent intensities in the jet.

The results of measurements of the shear-stress correlation coefficient, R_{uv}, in a turbulent wall jet by Eskinazi & Kruka (1962) and also in an axisymmetric jet by Gibson (1963) are compared with the present results in figure 18. The agreement is again quite good and supports the idea of a tendency towards a universally similar flow structure for all turbulent jet and wake flows.

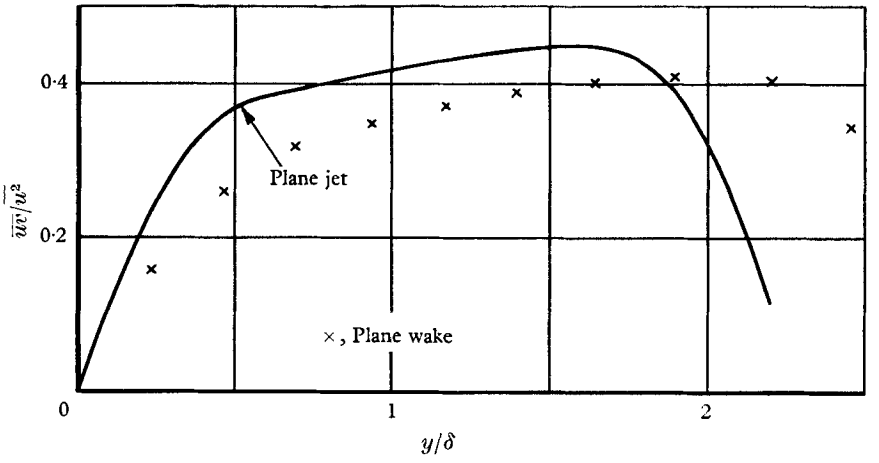

FIGURE 17. The distribution of $\overline{uv}/\overline{u^2}$ across the jet.

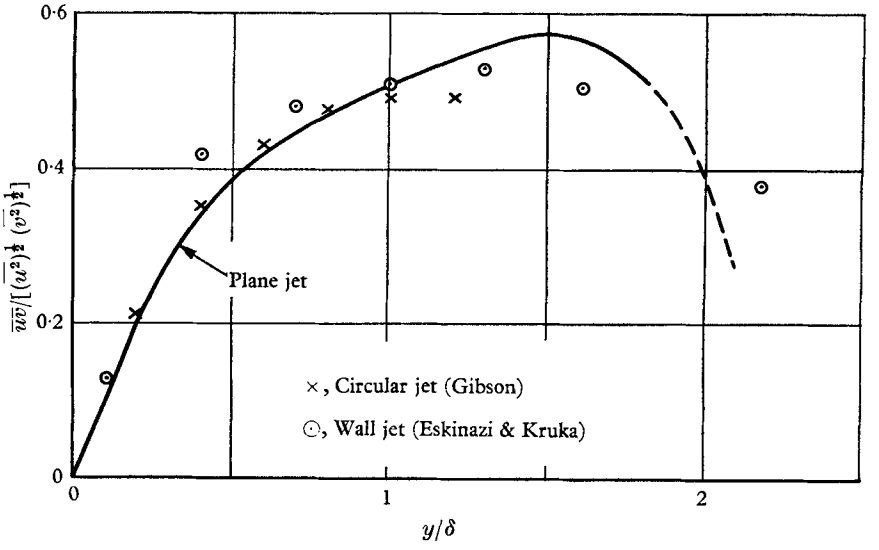

FIGURE 18. The shear-stress correlation coefficient distribution.

4.5. *The turbulent energy balance*

The turbulent energy balance may be written in the approximate form

$$\underbrace{\frac{U}{2}\frac{\partial\overline{q^2}}{\partial x}+\frac{V}{2}\frac{\partial\overline{q^2}}{\partial y}}_{\text{advection}}+\underbrace{\overline{uv}\frac{\partial U}{\partial y}}_{\substack{\text{production}\\ \text{from shear}\\ \text{stresses}}}+\underbrace{(\overline{u^2}-\overline{v^2})\frac{\partial U}{\partial x}}_{\substack{\text{production}\\ \text{from normal}\\ \text{stresses}}}+\underbrace{\frac{\partial}{\partial y}(\tfrac{1}{2}\overline{q^2v}+\overline{pv})}_{\text{diffusion}}+\underbrace{\epsilon}_{\text{dissipation}}=0,$$

where ϵ is the viscous dissipation of turbulent energy. If the distributions of the advection, production and dissipation terms are known, the distribution of the diffusion term can readily be obtained by difference. The advection and production terms were obtained from the turbulence measurements already described. The dissipation term was obtained by measuring the mean square of the time derivative of the u-component of velocity and using the expression

$$\epsilon = 15\nu\overline{(\partial u/\partial t)^2}.$$

This expression assumes that the eddies primarily responsible for the dissipation are isotropic and move with the local mean velocity. In the present experiments, it was found that the frequencies of the dissipating eddies extended up to and beyond 15 kc/s and it is certain that wire-length effects and possibly inadequate compensation in this frequency range led to values of the viscous dissipation that were much too small. Nevertheless, the energy balance has been obtained by suitably scaling the measured values of viscous dissipation to ensure in the final energy balance that

$$\int_0^\infty \frac{\partial}{\partial y}(\tfrac{1}{2}\overline{q^2 v} + \overline{pv})\,dy = 0,$$

i.e. the net diffusion of turbulent energy across the flow is zero. The resulting energy balance is shown in figure 19. It proved necessary to scale the measured distribution of the viscous dissipation by a factor of nearly two in order to obtain a sensible energy balance.

The main features of the energy balance are:

(i) The distribution of the viscous dissipation term is very similar to that found in a wake by Townsend and shows that, over the central portion of the flow, this term is roughly constant. By making an allowance for the intermittency factor, the region of approximately constant viscous dissipation is extended further.

(ii) The viscous dissipation and production terms are the most significant in the energy balance. This may be illustrated by comparing the integral values of the various terms in the energy balance over the jet width given in table 1.

(iii) Unlike the wake flow, it appears that the diffusion of turbulent energy $(\frac{1}{2}\overline{q^2 v} + \overline{pv})$ is at least roughly correlated with the local mean intensity gradient.

The micro-scale of the turbulence $\lambda = [\overline{u^2}/\overline{(\partial u/\partial x)^2}]^{\frac{1}{2}}$ can be calculated from the viscous dissipation term and, as shown in figure 20, the distribution of this length scale across the jet is again very similar to that found in a wake flow.

It is interesting to check the validity of the local isotropy assumption involved in the present measurements of viscous dissipation. According to Corrsin (1957), it is necessary that two conditions should be fulfilled. These are

$$(a)\quad \frac{(\epsilon/\nu)^{\frac{1}{2}}}{\partial U/\partial y} \gg 1{\cdot}0, \quad \text{and} \quad (b)\quad \frac{(\epsilon/\nu^3)^{\frac{1}{4}}}{(\overline{v^2})^{-\frac{1}{2}}\,\partial U/\partial y} \gg 1{\cdot}0.$$

The first condition is simply a requirement that the rate of strain due to the dissipating eddies be much larger than that due to the mean velocity gradient and the other condition is a requirement that the wave-numbers of the dissipating

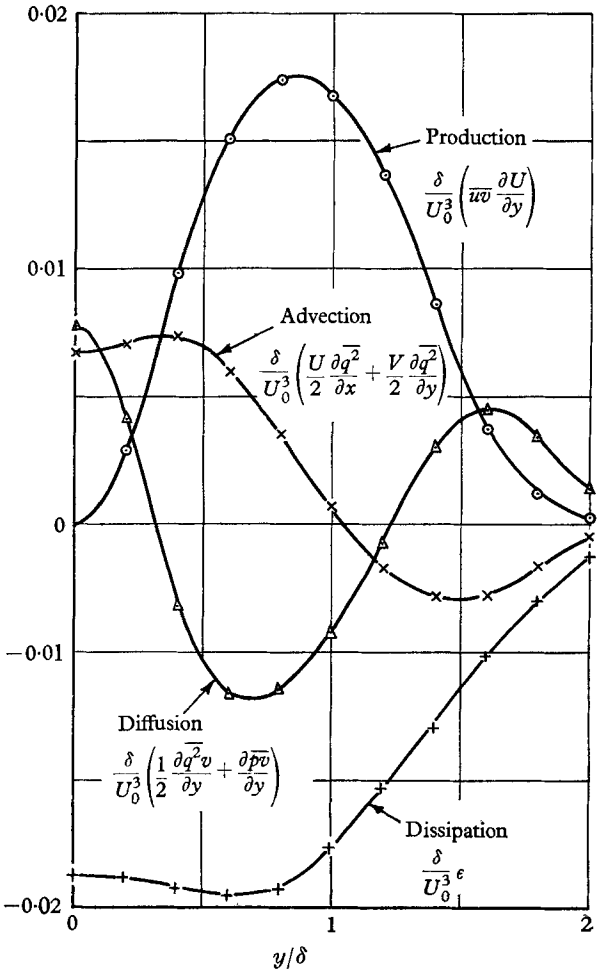

FIGURE 19. The turbulent energy balance.

Production	$\frac{\delta}{U_0^3}\int_0^\infty \overline{uv}\frac{\partial U}{\partial y}\,dy$	−0·0169
Dissipation	$\frac{\delta}{U_0^3}\int_0^\infty \epsilon\,dy$	+0·0207
Advection	$\frac{\delta}{U_0^3}\int_0^\infty \left(\frac{U}{2}\frac{\partial\overline{q^2}}{\partial x}+\frac{V}{2}\frac{\partial\overline{q^2}}{\partial y}\right)dy$	−0·0038
Diffusion	$\frac{\delta}{U_0^3}\int_0^\infty \frac{\partial}{\partial y}(\frac{1}{2}\overline{q^2v}+\overline{pv})\,dy$	0

TABLE 1

eddies be much larger than those at which energy is fed into the turbulence. For the present measurements, it is found that

$$(a)\quad \frac{(\epsilon/\nu)^{\frac{1}{2}}}{\partial U/\partial y} = 24, \quad \text{and} \quad (b)\quad \frac{(\epsilon/\nu^3)^{\frac{1}{4}}}{(\overline{v^2})^{-\frac{1}{2}}\,\partial U/\partial y} = 125.$$

Thus the use of the simplified expression for the viscous dissipation term would seem well justified.

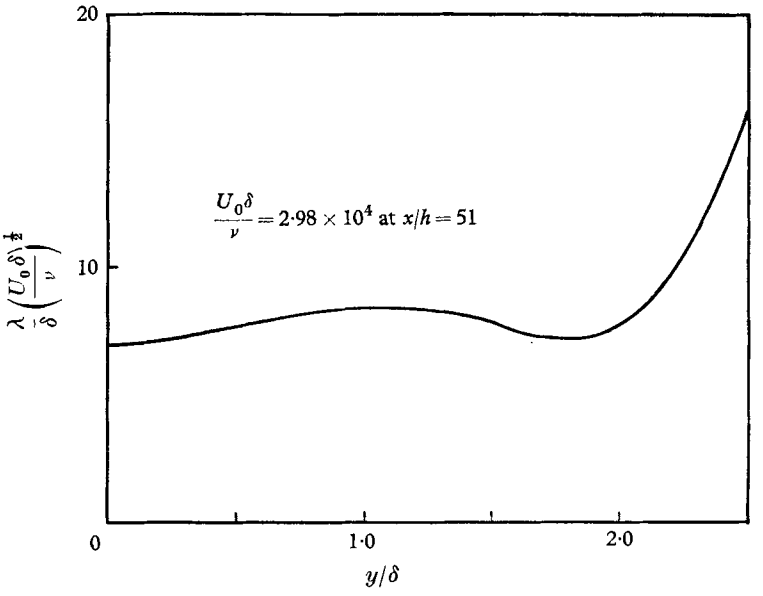

FIGURE 20. The micro-scale of the turbulence.

4.6. *The eddy structure*

Townsend has postulated what is essentially a double structure for shear flows. The largest eddies appear to be 'jets' of fluid that originate at the boundary of the strained turbulent fluid with the non-turbulent fluid and which erupt outwards (Grant 1958). It is these eddies that appear responsible for the intermittency phenomenon. The remaining turbulence is assumed to be about one-tenth of the scale of the large eddies and to contain between 80 and 90 % of the turbulent energy. These smaller eddies are also assumed to be primarily responsible for the shear stress. From this model, Townsend has built up a convincing model of turbulent shear flows which enables the value of the eddy viscosity coefficient to be predicted roughly and which also explains the difference between the values of this eddy viscosity coefficient in jet and wake flows. However, in spite of his extensive experimental studies of the wake flow structure, the validity of his model is not yet firmly established and a great deal more work is required to clarify the precise nature of the turbulence structure. In the present experiments, a few correlation-coefficient and spectrum measurements were made which, although they are in no way comprehensive, are worth reporting in so far as they may add to the information on this eddy-structure problem. The measurements

were carried out in the jet at $y/\delta = 0{\cdot}5$ and $x/h = 50$ and they consisted of measurements of the lateral correlation-coefficient $R_{11}(0, r, 0)$, subsequently referred to as R_y, and some $\overline{u^2}$- and $\overline{uv}$-spectra measurements.

The correlation coefficient measurements were obtained with one wire fixed at $y/\delta = 0{\cdot}5$ and the other wire traversed outwards towards the edge of the jet. In order to obtain some idea of the length scales appropriate to the various frequencies, these correlation measurements were obtained by passing the various

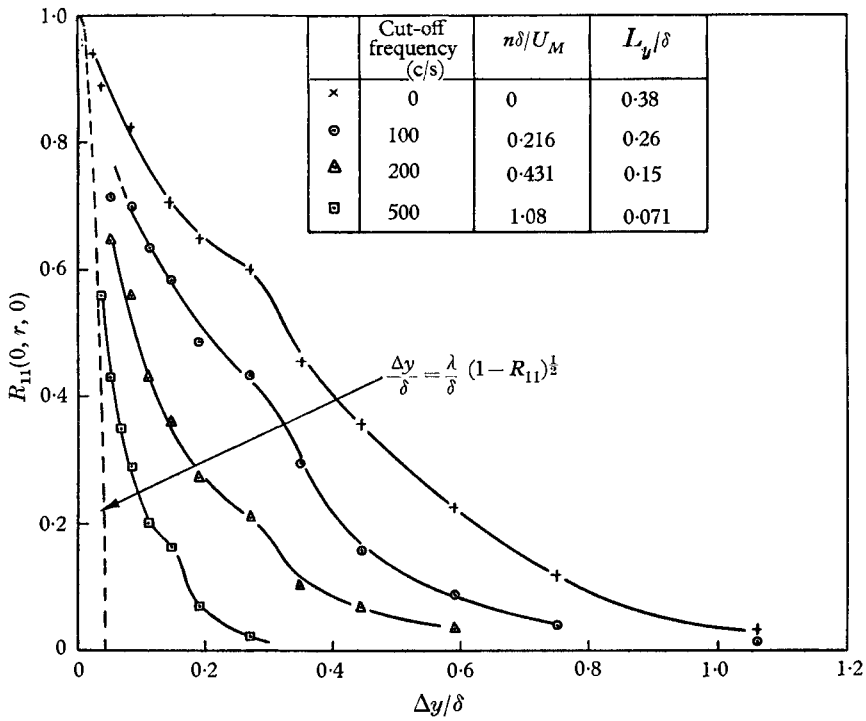

FIGURE 21. Filtered lateral correlation coefficients.

signals through a variable high-pass filter unit and measuring the outputs for different settings of the filter. The resulting correlation coefficients are shown in figure 21. Before discussing these filtered correlation measurements, the overall lateral integral scale

$$L_y = \int_0^\infty R_y \, dy$$

will be compared with the values found in other free turbulent flows. Since the mean velocity profiles in all these flows are roughly similar, it is possible to use δ as a reference length for the width of the shear layer in every case. In addition to a comparison of values of L_y, table 2 also compares values of the longitudinal integral scale

$$L_x = \int_0^\infty R_x \, dx,$$

where values are available.

Although the data is not very complete, it seems that the longitudinal integral scale L_x is very roughly constant for all the flows considered but the lateral scale is smaller in jets than it is in wakes. This is consistent with the idea that the comparatively large lateral velocities found in jets but not in wakes inhibit the growth of the large eddies in the lateral direction.

Flow	Author	L_y/δ	L_x/δ	L_x/L_y
Isotropic turbulence	Theoretical result	—	—	2·0
Plane jet	Present measurements	0·38	—	—
Plane wake	Townsend (1956)	0·6	0·83	1·37
Plane wake	Grant (1958)	0·5	0·83	1·66
Mixing layer	Liepmann & Laufer (1947)	0·26	—	—
Mixing layer	Laurence (1956)	—	—	2·5–3·0
Circular jet	Corrsin (1943)	0·23	—	—
Circular jet	Corrsin & Uberoi (1949)	0·17	0·92	5·4
Circular jet	Gibson (1963)	—	0·95	—

TABLE 2

In order that the results of the spectrum measurements may be compared with any future measurements in a plane jet in still air, a frequency parameter has been used which is given by $\Omega = n\delta/U_M$, where n is the frequency and U_M is the average mean velocity across the jet, $U_1 + 0{\cdot}5U_0$. In a truly self-preserving plane jet in still air, there would be no ambiguity if the velocity in the frequency parameter was chosen as U_0 but, where the free-stream velocity is not exactly zero, it is perhaps better to use U_M as it has been shown by Davies, Fisher & Barratt (1963) that the average convection velocity of the turbulence in the mixing layer of a jet is not very different from this average mean velocity U_M. The spectrum measurements were obtained by passing the hot-wire anemometer signals through a variable high-pass filter and measuring the mean-square output voltages for a range of settings of the filter. If $\overline{u^2}F(\Omega)$ and $\overline{uv}G(\Omega)$ represent the contributions to $\overline{u^2}$ and $\overline{uv}$ respectively, from frequencies between Ω and $\Omega + d\Omega$, then the outputs from the filter unit gave

$$\int_0^{\Omega'} F(\Omega)\,d\Omega \quad \text{and} \quad \int_0^{\Omega'} G(\Omega)\,d\Omega,$$

where Ω' is the effective setting of the high-pass filter. These latter quantities are shown in figure 22. The most obvious feature of these results is the fact that the shear-stress spectrum approaches zero more rapidly than the $\overline{u^2}$ spectrum. This is a well-known phenomenon and shows that there is a range of eddies which do not contribute anything to the shear stress. This is a necessary condition for the existence of local isotropy and shows that the turbulence structure was not obviously inconsistent with this hypothesis. The results also show that the eddies primarily responsible for both the major part of the shear stress and turbulent energy are contained in a frequency range from $\Omega = 0$ to $\Omega = 0{\cdot}3$. The filtered correlation measurements show that when the high-pass filter was set to a frequency equivalent to $\Omega = 0{\cdot}22$, the lateral integral scale was reduced by only about 30 % to a value of $L_y/\delta = 0{\cdot}26$. This suggests that a large portion

of the turbulent shear stress and energy is carried by eddies which are quite large in comparison with the width of the shear layer. This is in accord with recent and far more comprehensive measurements of Bradshaw *et al.* (1963) and suggests that Townsend's separation of large- from shear-carrying eddies may not be a particularly valid assumption.

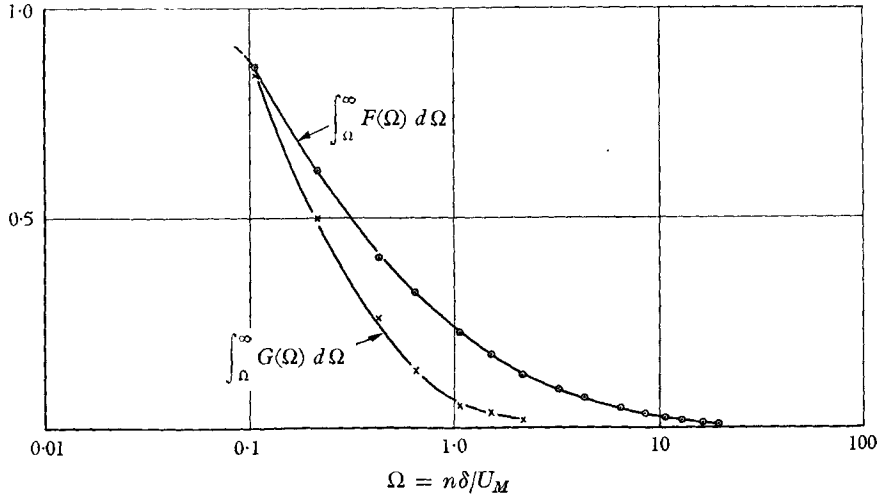

FIGURE 22. The shear stress and $\overline{u^2}$ spectrum.

Some experiments were also carried out in which the average frequency of the pulses from the intermittency meter was measured.† This was an extremely crude experiment and these average frequencies may be as much as 50 % in error. Nevertheless, the results may be of interest and, so that their significance can be understood more easily, an imaginary case will first be considered in which the boundary of the turbulent flow is in the form of a sine wave travelling with the average mean velocity of the flow, U_M. Now, in the imaginary flow, the outputs from the intermittency meter at different positions in the intermittent region would be similar to those shown in figure 23(*b*). The frequency meter (which was, in practice, a pulse counter) would give a constant value of the frequency in the intermittent region, say n, and zero frequency in the fully-turbulent or non-turbulent flow, as in figure 23(*c*). This frequency may be used to define an eddy wavelength, U_M/n. If these eddies are to be consistent with self-preservation, their wavelengths should be a constant proportion of the jet width so that the distribution of the parameter $n\delta/U_M$ across the jet should be independent of the longitudinal station. The results of the present measurements are shown in figure 24 and they show that, although the accuracy of the measurements is poor, the results are not obviously in contradiction with self-preservation of the eddies responsible for intermittency. Further, since the turbulence is made up of a whole spectrum of eddies, the frequency distribution is not 'square'. Nevertheless, we may take the maximum value of the parameter $\delta n/U_M$ to give

† The duration of each pulse corresponded to the duration of a 'burst' of turbulence.

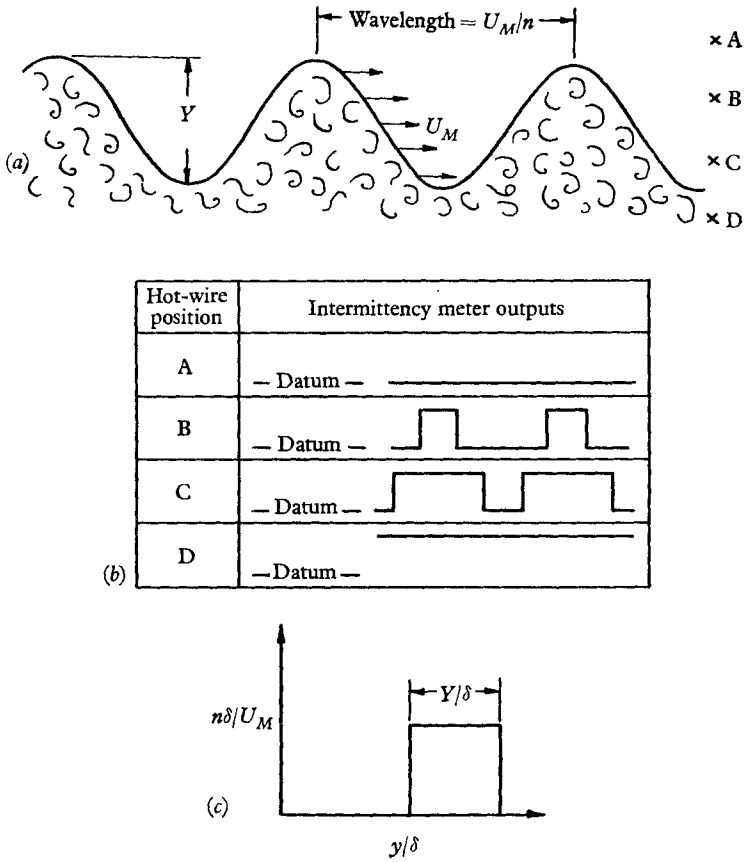

FIGURE 23. Frequency measurements of intermittency for a turbulent flow, with a sinusoidal boundary. (*a*) Schematic representation of intermittent region. (*b*) Signals from the intermittency meter. (*c*) Frequency measurements in the intermittent region.

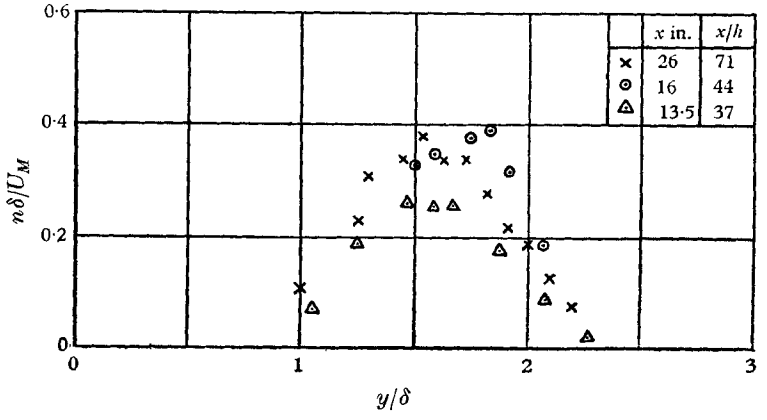

FIGURE 24. Frequency of eddies responsible for intermittency.

an idea of the average frequency and wavelength of the eddies responsible for intermittency. On this basis

$$n\delta/U_M = 0{\cdot}3 \pm 0{\cdot}1.$$

Now, from the spectrum measurements previously discussed, it appeared that the bulk of the shear stress and turbulent energy was contained in the frequency range from $\Omega = 0$ to $\Omega = 0{\cdot}3$, and this seems to suggest that the eddies responsible for intermittency are also responsible for a large portion of the shear stress. It is appreciated that the interpretation put upon the present results is not free from objections particularly regarding the use of a single velocity U_M to compare measurements at different points across the jet; nevertheless, combined with the results of previous investigators, this provides mounting evidence to suggest that the shear-carrying eddies are among the larger eddies in the flow and, in fact,

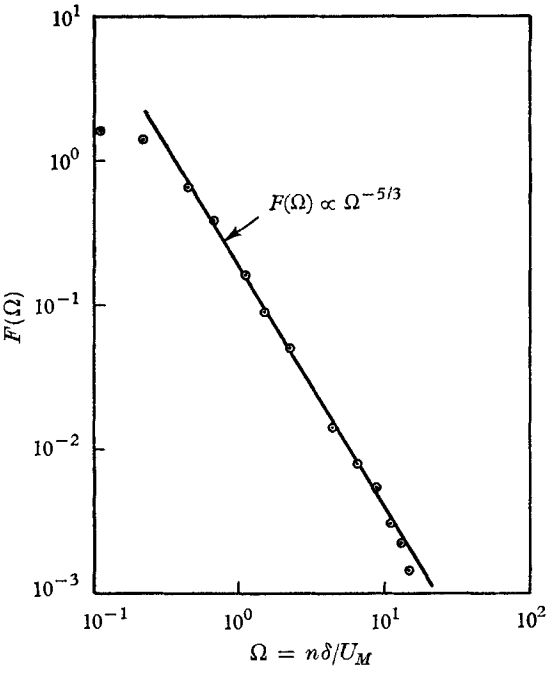

FIGURE 25. $\overline{u^2}$ spectrum showing an inertial subrange.

may be among those eddies responsible for intermittency. This suggestion is contrary to Townsend's large-eddy hypothesis and is clearly a matter requiring further attention. There is a good deal of evidence to show that mechanisms at least similar to those proposed by Townsend are at work in turbulent shear flows, and it may be that his flow model can be made more adequate if some allowance can be made for the contributions from the large eddies to the overall shear stress. However, more experimental work is required before any such modifications can be contemplated with confidence.

To return to the spectrum measurements, the one-dimensional spectrum function $F(\Omega)$ has been obtained by differentiating graphically the results of figure 22. Although this is not a very accurate procedure, this spectrum function,

shown in figure 25, clearly exhibits an inertial subrange region in which $F(\Omega) \propto \Omega^{-\frac{5}{3}}$. The condition necessary for the existence of an inertial subrange is that there should be a region in wave-number space which contributes very little either to the turbulent energy or to the viscous dissipation. This requires a very high Reynolds number and it has been suggested that $R_\lambda = (\overline{u^2})^{\frac{1}{2}}\lambda/\nu$ should not be less than 500 (see Gibson 1963). In the present experiments, the value of R_λ was about 350 and the separation between energy-containing eddies and those responsible for viscous dissipation seems to have been large enough to permit the existence of a limited inertial subrange. The Universal Equilibrium theory (see, for example, Hinze 1959) shows that, in the inertial subrange, the spectrum function is given by

$$\overline{u^2}F(k) = \tfrac{18}{55}A\,\epsilon^{\frac{2}{3}}k^{-\frac{5}{3}},$$

where A is a universal constant and k is the wave-number. The present results give $A = 1{\cdot}54$, which is in good agreement with the value of 1·6 obtained by Gibson (1963) in a circular jet and the value of 1·44 obtained by Grant, Stewart & Moilliet (1962) in a tidal channel.

4.7. *The unsteady irrotational flow*

The convoluting edge of a turbulent flow induces unsteady but irrotational velocity fluctuations in the free stream. According to Phillips (1955) and Stewart (1956), the components of this unsteady motion are related to one another such that

$$\overline{v^2} = \overline{u^2} + \overline{w^2}.$$

Furthermore, at large distances from the edge of the turbulent flow, it is found that

$$\tfrac{1}{2}\overline{v^2} = \overline{u^2} = \overline{w^2}\alpha(y - y_0)^{-4},$$

where y_0 is the apparent origin of these irrotational fluctuations. Measurements of the $\overline{u^2}$ component confirm the validity of this expression for this term as shown by figure 26. This data is well represented for $y/\delta \geqslant 2{\cdot}3$ by the expression

$$u^2/U_0^2 = 0{\cdot}0016[(y - y_0)/\delta]^{-4},$$

where $y_0/\delta = 1{\cdot}33 \pm 0{\cdot}03$. It is to be noted that the apparent origin of the fluctuations, y_0/δ, lies well within the region where turbulent flow exists: the intermittency factor is approximately 0·8 at $y/\delta = 1{\cdot}33$. It is also to be noted that the above expression for $\overline{u^2}/U_0^2$ appears to be valid even quite close to the edge of the jet, although the theories suggest that its form is only asymptotically correct for large values of y/δ. This was found to be true also in the case of wake flow (see Phillips 1955).

The $\overline{v^2}$ and $\overline{w^2}$ intensities in the irrotational-flow region were obtained with a single sloping hot-wire which measured the quantity $\overline{u^2} + \alpha(\overline{v^2}$ or $\overline{w^2})$, where α is a constant for any given hot-wire (see § 3). In order to determine the ratios $\overline{v^2}/\overline{u^2}$ and $\overline{w^2}/\overline{u^2}$, it was assumed that

$$\frac{\overline{u^2}}{U_0^2} = k_u\left(\frac{y - y_0}{\delta}\right)^{-4}, \quad \frac{\overline{v^2}}{U_0^2} = k_v\left(\frac{y - y_0}{\delta}\right)^{-4}, \quad \text{and} \quad \frac{\overline{w^2}}{U_0^2} = k_w\left(\frac{y - y_0}{\delta}\right)^{-4}.$$

Thus, from the measurements with the single sloping wire, we have

$$\overline{u^2}/U_0^2+\alpha\overline{v^2}/U_0^2 = (k_u+\alpha k_v)\,[(y-y_0)/\delta]^{-4},$$

and another similar expression containing $\overline{w^2}$. From the experimental results, graphs of $[\overline{u^2}/U_0^2+\alpha\overline{v^2}/U_0^2]^{-\frac{1}{4}}$ and $[\overline{u^2}/U_0^2+\alpha\overline{w^2}/U_0^2]^{-\frac{1}{4}}$ have been plotted against $(y-y_0)/\delta$ from which values of $k_u+\alpha k_v$ and $k_u+\alpha k_w$ have been obtained. The final results of the measurements at a number of longitudinal stations are given in table 3. Considering the inherent lack of accuracy of the single sloping-wire technique, these results can be regarded as providing satisfactory confirmation of the predictions of the theories of Phillips and Stewart.

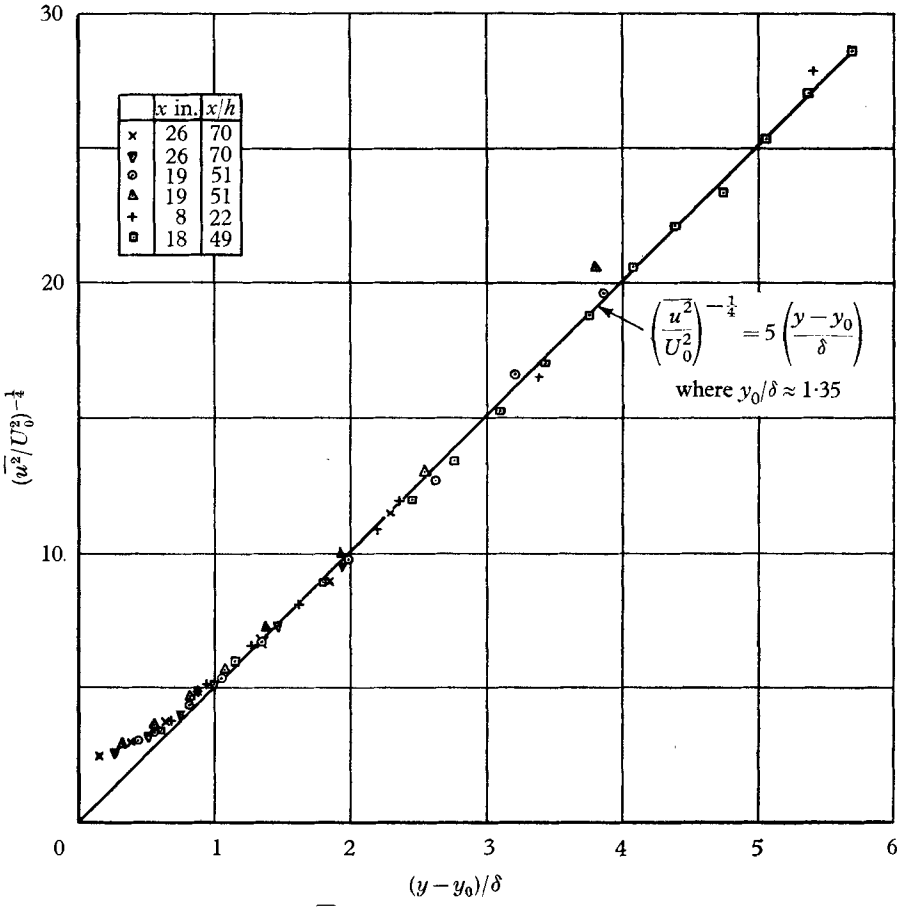

FIGURE 26. $\overline{u^2}$ distribution in the irrotational flow.

x/h	α	$k_u+\alpha k_v$	$k_u+\alpha k_w$	k_v/k_u	k_w/k_u
48·5	0·593	0·00355	0·00275	2·06	1·21
51	0·84	0·00345	0·0026	1·38	0·75
70	0·41	0·00355	0·00225	3·0	1·02
			Average values	2·5	1·0

TABLE 3

5. The applicability of the various simple theories of turbulence

Both the constant-exchange hypothesis and the mixing-length theories postulate a gradient transport mechanism, but this is not the only type of transport mechanism that is possible in turbulent shear flows. Townsend (1956) and Batchelor (1950) have considered a model flow in which the transport process may be represented as the sum of a gradient transport mechanism and a bulk transport mechanism. This model is in keeping with Townsend's suggestion that the turbulent eddies may be divided roughly into two groups, namely the large eddies which will be responsible for the bulk transport, and the much smaller energy containing eddies which will be responsible for the gradient transport mechanism. For this model, we may write

$$\overline{\theta v} = \overline{\theta}\overline{V} + K\,\partial\overline{\theta}/\partial y,$$

where $\overline{\theta}$ is the average value of the transported property, $\overline{V}$ is the average value of the bulk transport velocity and K is a gradient diffusion coefficient. On a qualitative basis, Townsend was able to explain many of the observed features of a turbulent shear flow with this model, but difficulties arise when quantitative use of the model is attempted. The relative importance of the bulk and gradient-transport mechanisms depends on the nature of the property transported and there remains the problem of attaching values to the bulk transport velocity and the gradient diffusion coefficient. This lack of precision in this model makes a detailed comparison with experimental data difficult and, in the present case, we shall restrict ourselves to the more straightforward comparison with the simple gradient transport theories.

5.1. *The constant-exchange hypothesis*

For the constant-exchange hypothesis to have any physical validity, it is necessary that the turbulence structure be reasonably homogeneous across the jet and also that $(\overline{q^2})^{\frac{1}{2}}/L \gg \partial U/\partial y$, where L is a representative length scale of the turbulence. Now, although the fine structure of the turbulence is apparently closely homogeneous across the width of the flow, reference to the distribution of turbulent energy (figure 15) shows that homogeneity of the energy-containing eddies cannot be regarded as a particularly good assumption although, at the same time, it is not wholly unreasonable over the central portion of the flow and it has been argued that the 'stirring' action of the largest eddies will tend to ensure a roughly homogeneous turbulence structure. However, the discovery that $((\overline{q^2})^{\frac{1}{2}}/L_y)/(\partial U/\partial y) = O(1)$ is sufficient to show that the constant exchange hypothesis cannot have any real physical validity. Notwithstanding this last point, the hypothesis remains a useful empiricism and if we calculate the distribution of eddy viscosity across a plane jet including an allowance for the intermittency factor, we find that over an appreciable region of the flow, the eddy viscosity coefficient is roughly constant (see figure 27).†

† Figure 27 shows the distribution of the reciprocal of the eddy Reynolds number $1/R_T = \nu_T/U_0\delta = g_{12}(\eta)/f'(\eta)$ and also $1/\gamma R_T$. The calculations were made for $U_1 = 0$ and $d\delta/dx = 0{\cdot}109$ for simplicity.

5.2. *Prandtl's mixing-length theory*

In the case of Prandtl's mixing-length theory, it is necessary that $(\overline{u^2})^{\frac{1}{2}}/L \approx dU/dy$ and that the turbulent velocity fluctuations should be similar throughout the flow, i.e. parameters like $\overline{v^2}/\overline{u^2}$, etc. and R_{uv} should be constants.

If we calculate the distribution of the mixing length across the jet by assuming that

(*a*) $L/\delta = \{(\overline{u^2})^{\frac{1}{2}}/\delta\}/(\partial U/\partial y) = g_1(\eta)/f'(\eta)$

and (*b*) $L/\delta = \{(\tau/\rho)^{\frac{1}{2}}/\delta\}/(\partial U/\partial y) = \{g_{12}(\eta)\}^{\frac{1}{2}}/f'(\eta)$,

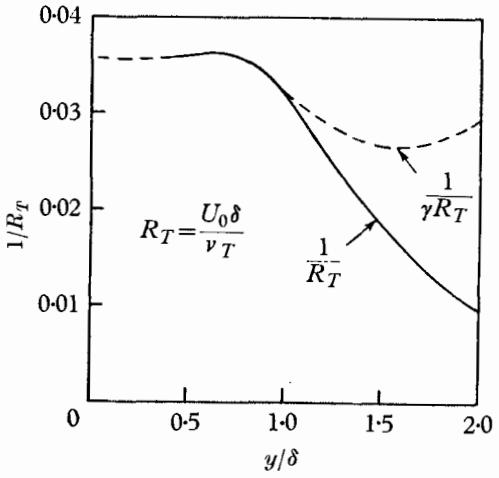

FIGURE 27. Eddy viscosity distribution across a plane jet.

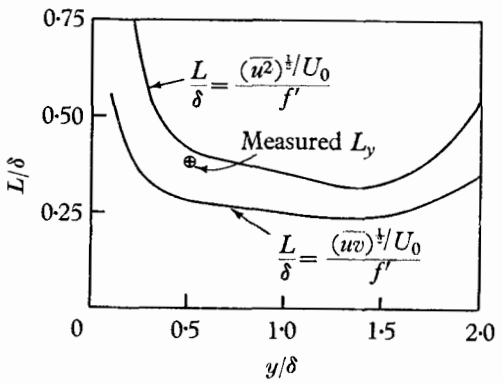

FIGURE 28. Mixing-length distribution across a plane jet.

we obtain the results shown in figure 28. With the obvious exception of the central region of the flow, both distributions show that the mixing length is roughly constant over the main portion of the jet and, moreover, it is interesting to note that the former relationship gives a value of $L/\delta \approx 0{\cdot}35$ which is in close agreement with the measured value of $L_y/\delta = 0{\cdot}38$. The numerical difference between the two calculated distributions of mixing length is not important since it arises from the fact that $R_{uv} \neq 1$ and $\overline{u^2} \neq \overline{v^2}$.

The validity of the flow similarity assumption can be tested by reference to figures 16, 17 and 18. As discussed earlier, these show that, except near the flow centre, the similarity assumption may not be wholly unreasonable although it is again not a very precise assumption either.

Finally, it has been shown by Batchelor (1950) that the Prandtl mixing-length theory requires an energy balance between the production and viscous dissipation of turbulent energy. Reference to the energy balance (figure 19) shows that, over a region of the flow, the production and dissipation terms are indeed predominant although the advection and diffusion terms are by no means negligible.

5.3. *Further comment on the theories of turbulence*

On balance, it seems that of the two simple gradient-transport theories discussed, the Prandtl mixing-length theory gives a slightly better description of the flow. However, this result does not necessarily have any far-reaching significance because it is restricted to the plane-jet flow. For example, in the plane wake, the energy balance between production and dissipation of turbulent energy implied in the mixing-length theory is not found. In any case, the structure of the jet flow does not obviously conform to any really well-defined pattern as witnessed by the comparative ease with which the experimental results have been shown to exhibit features associated with quite different assumptions about the flow. On the one hand, in connexion with the constant-exchange hypothesis, it was argued that the assumptions of a roughly constant value of turbulent energy across the jet and $\tau \propto \partial U/\partial y$ were not unreasonable. On the other hand, it was then shown that $(\overline{u^2})^{\frac{1}{2}} \propto L\,\partial U/\partial y$ and $\tau \propto (\partial U/\partial y)^2$ were also reasonable assumptions. This duplicity of interpretation is not uncommon in work on turbulence and it probably arises, to some extent, because the turbulence comprises a whole spectrum of eddies with their own length and time scales and which are subjected to different physical controlling factors. This diversity of eddy scales ensures that no single simple mechanism can be expected to describe the whole of the turbulence structure. Hence, where there is apparently a measure of support from the experimental work for two different assumptions, it may well be that both assumptions apply but to different ranges of eddy size. In fact, it is clear that to be able to make progress on the turbulence problem, it is necessary to split the turbulence into groups of eddies (even though this in itself is artificial) with more or less distinct scales of length and time and to then construct theories or mechanisms to account for the behaviour of each eddy group and also its interaction, if any, with other eddy groups. This is, of course, precisely the approach used in the theories of the dissipating range of eddies and also used by Townsend in his large-eddy hypothesis.

In conclusion, it is interesting to reconsider very briefly the flow structure in the light of the experiments of Grant (1958) and some of the present results. According to Grant, the most obvious large-scale motions in a wake are 'a series of more or less regularly spaced "jets" of turbulent fluid proceeding outwards from the central plane of the wake'. Motions similar to those described by Grant can often be seen in jets of steam and in smoke from chimneys and they are

clearly responsible for intermittency. Now, it has been suggested earlier that these large eddies may contain a considerable portion of the turbulent energy and shear stress and it is interesting to note that these jet-like motions would give rise to a distribution of the $(\overline{u^2})^{\frac{1}{2}}$ intensity similar to that postulated by the Prandtl mixing-length theory, provided the lateral velocity with which the jets grew was large enough to prevent appreciable diffusion of the fluid within the jets during the course of their development. If this last condition were fulfilled, and the eddies were responsible for a large part of the shear, we could expect that a high instantaneous value of the shear stress would be accompanied by a higher than average value of the v-component of velocity. This suggests that a test of these ideas would be provided by measurements of the quantity $\overline{u^2v}/\overline{uv}(\overline{v^2})^{\frac{1}{2}}$, which should be much greater than 1·0 if the above ideas were correct. Obviously measurements of this sort would not be enough and there is still a great need for further correlation and spectrum measurements including, perhaps, some more careful measurements using the signals from an intermittency meter of the sort used in the present tests.

6. Conclusions

The results of the turbulence measurements have shown that self-preservation in a turbulent plane jet is established at distances from the jet nozzle greater than thirty jet nozzle widths. In the self-preserving region of the jet flow, the distributions of the turbulent intensities and shear stress are found to be very similar to those found in a plane wake by Townsend. This suggests that there may be some tendency towards a universal structure for all turbulent free flows. The major differences between the plane jet and wake, which were partly anticipated by Townsend, were that the large eddies in the plane jet were somewhat smaller than those found in the plane wake and, also, the turbulent energy balance for the plane jet showed a greater contribution from the production and dissipating terms than in the case of a plane wake. The structure of the small-scale eddies responsible for the viscous dissipation appeared to be constant over the central portion of the jet width and all the indications were that it was closely isotropic. In fact, some evidence was found suggesting the existence of an inertial subrange. As far as the shear-carrying eddies were concerned, it appeared that these were among the largest eddies in the flow and responsible, in part at least, for the intermittency phenomenon. This conclusion is contrary to Townsend's large eddy hypothesis and is a matter that deserves additional attention. It was found that the assumption of a nearly uniform level of turbulent energy across the jet was not a particularly good assumption since it proved possible to represent the distribution of the $(\overline{u^2})^{\frac{1}{2}}$ intensity quite well by the Prandtl mixing-length hypothesis thus showing a strong correlation between the turbulent energy and the mean velocity gradient. Finally, the irrotational velocity fluctuations outside the jet bore out the conclusions of the theories of Phillips (1955) and Stewart (1956), and the anomalies between these theories and the experimental work of Corrsin (1943) on a circular jet would seem now to be almost certainly caused by instrumentation errors.

The author would like to thank Prof. A. D. Young and the staff of the Aeronautical Engineering Department at Queen Mary College for their help and encouragement during the course of this research. Thanks are also due to the Department of Scientific and Industrial Research for the provision of a grant.

REFERENCES

BATCHELOR, G. K. 1950 Note on free turbulent flows with special reference to the two-dimensional wake. *J. Aero. Sci.* **17**, 441.

BRADBURY, L. J. S. 1963 An investigation into the structure of a turbulent plane jet. Ph.D. thesis, University of London.

BRADBURY, L. J. S. 1964 A simple circuit for the measurement of the intermittency factor in a turbulent flow. *Aero. Quart.* **15**, 281.

BRADSHAW, P., FERRISS, D. H. & JOHNSON, R. F. 1963 Turbulence in the noise producing region of a circular jet. *N.P.L. Aero. Rep.* no. 1054.

COLLIS, R. D. & WILLIAMS, M. J. 1959 Two-dimensional convection from heated wires at low Reynolds numbers. *J. Fluid Mech*, **6**, 357.

CORRSIN, S. 1943 An investigation of the flow in an axially symmetric heated jet. *NACA Rep.* no. W-94.

CORRSIN, S. 1957 Some current problems in turbulent shear flows. *Nat. Acad. Sci. Naval Hydrodynamics, Publ.* no. 515.

CORRSIN, S. & KISTLER, A. L. 1954 The free-stream boundaries of turbulent flow. *NACA TN* no. 3133.

CORRSIN, S. & UBEROI, M. 1949 Further experiments on the flow and heat transfer in a heated turbulent air jet. *NACA TN* no. 1865.

DAVIES, P. A. O. L., FISHER, M. J. & BARRATT, M. J. 1963 The characteristics of the turbulence in the mixing region of a round jet. *J. Fluid Mech.* **15**, 337.

ESKINAZI, S. & KRUKA, V. 1962 Turbulence measurements in a two-dimensional rectangular wall jet with longitudinal free-stream. *Syracuse Univ. Res. Inst. Rep.* no. ME 937-6205P.

FORTHMANN, E. 1936. Turbulent jet expansions. *NACA TM* no. 789.

GIBSON, M. M. 1963 Spectra of turbulence in a round jet. *J. Fluid Mech.* **15**, 161.

GRANT, H. L. 1958 The large eddies of turbulent motion. *J. Fluid Mech.* **4**, 149.

GRANT, H. L., STEWART, R. W. & MOILLIET, A. 1962 Turbulence spectra from a tidal channel. *J. Fluid Mech.* **12**, 241.

HINZE, J. O. 1959 *Turbulence.* New York: McGraw Hill Book Co.

KLEBANOFF, P. S. 1954 Characteristics of turbulence in a boundary layer with zero pressure gradient. *NACA TN* no. 3178.

LAURENCE, J. C. 1956 Intensity, scale and spectra of turbulence in the mixing region of a free subsonic jet. *NACA Rep.* no. 1292.

LIEPMANN, H. W. & LAUFER, J. 1947 Investigation of free turbulent mixing. *NACA TN* no. 1257.

MILLER, D. R. & COMMINGS, E. W. 1957 Static pressure distribution in the free turbulent jet. *J. Fluid Mech.* **3**, 1.

NAKAGUCHI, H. 1961 Jet along a curved wall. *Tokyo University Aerodynamics Res. Memo.* no. 4.

NEWMAN, B. G. & LEARY, B. G. 1949 The measurement of the Reynolds stresses in a circular pipe as a means of testing a hot-wire anemometer. *Rep. Dept. Supply, Aero Res. Lab.* no. A 72.

PHILLIPS, O. 1955 The irrotational motion outside a free turbulent boundary. *Proc. Camb. Phil. Soc.* **51**, 220.

RUETNIK, J. R. 1955 The effect of the temperature dependence of King's constant A on the hot wire sensitivity coefficient. *J. Aero. Sci.* **22**, 502.

STEWART, R. W. 1956 Irrotational motion associated with free turbulent flows. *J. Fluid Mech.* **1**, 593.

TOOMRE, A. 1960 Effect of turbulence on static pressure measurements. *Aero Res. Counc. FM* no. 2972.

TOWNSEND, A. A. 1956 *The Structure of Turbulent Shear Flow.* Cambridge University Press.

VAN DER HEGGE ZIJNEN, B. G. 1958*a* Measurements of the velocity distribution in a plane turbulent jet of air. *Appl. Sci. Res.* A, **7**, 256.

VAN DER HEGGE ZIJNEN, B. G. 1958*b* Measurements of the distribution of heat and matter in a plane turbulent jet of air. *Appl. Sci. Res.* A, **7**, 277.

VAN DER HEGGE ZIJNEN, B. G. 1958*c* Turbulence measurements in a two-dimensional jet. *Appl. Sci. Res.* A, **7**, 293.

WEBSTER, C. A. G. 1962 A note on the sensitivity to yaw of a hot wire anemometer. *J. Fluid Mech.* **13**, 307.